Reinforced Concrete Foundation Remote Monitoring

FDOT Contract Number: BDV34-977-09

January 2019

Final Report

Prepared by:

Brian Kopp

Juan Aceros

Adel K El Safty

The University of North Florida

DISCLAIMER PAGE

The opinions, findings, and conclusions expressed in this publication are those of the authors and not necessarily those of the State of Florida Department of Transportation.

The contents of this report reflect the views of the authors, who are responsible for the facts and the accuracy of the information presented herein. This document is disseminated under the sponsorship of the Department of Transportation's University Transportation Centers Program, in the interest of information exchange. The U.S. Government assumes no liability of the contents or use thereof.

APPROXIMATE CONVERSIONS TO SI UNITS

SYMBOL	WHEN YOU KNOW	MULTIPLY BY	TO FIND	SYMBOL
LENGTH				
in	inches	25.4	millimeters	mm
ft	feet	0.305	meters	m
yd	yards	0.914	meters	m
mi	miles	1.61	kilometers	km
SYMBOL	**WHEN YOU KNOW**	**MULTIPLY BY**	**TO FIND**	**SYMBOL**
AREA				
in^2	square inches	645.2	square millimeters	mm^2
ft^2	square feet	0.093	square meters	m^2
yd^2	square yard	0.836	square meters	m^2
ac	acres	0.405	hectares	ha
mi^2	square miles	2.59	square kilometers	km^2
SYMBOL	**WHEN YOU KNOW**	**MULTIPLY BY**	**TO FIND**	**SYMBOL**
VOLUME				
fl oz	fluid ounces	29.57	milliliters	mL
gal	gallons	3.785	liters	L
ft^3	cubic feet	0.028	cubic meters	m^3
yd^3	cubic yards	0.765	cubic meters	m^3
NOTE: volumes greater than 1000 L shall be shown in m^3				
SYMBOL	**WHEN YOU KNOW**	**MULTIPLY BY**	**TO FIND**	**SYMBOL**
MASS				
oz	ounces	28.35	grams	g
lb	pounds	0.454	kilograms	kg
T	short tons (2000 lb)	0.907	megagrams (or "metric ton")	Mg (or "t")
SYMBOL	**WHEN YOU KNOW**	**MULTIPLY BY**	**TO FIND**	**SYMBOL**
TEMPERATURE (exact degrees)				
°F	Fahrenheit	5 (F-32)/9 or (F-32)/1.8	Celsius	°C
SYMBOL	**WHEN YOU KNOW**	**MULTIPLY BY**	**TO FIND**	**SYMBOL**
ILLUMINATION				
fc	foot-candles	10.76	lux	lx
fl	foot-Lamberts	3.426	$candela/m^2$	cd/m^2
SYMBOL	**WHEN YOU KNOW**	**MULTIPLY BY**	**TO FIND**	**SYMBOL**
FORCE and PRESSURE or STRESS				
lbf	pound force	4.45	newtons	N
lbf/in^2	pound force per square inch	6.89	kilopascals	kPa

APPROXIMATE CONVERSIONS TO ENGLISH UNITS

SYMBOL	WHEN YOU KNOW	MULTIPLY BY	TO FIND	SYMBOL
LENGTH				
mm	millimeters	0.039	inches	in
m	meters	3.28	feet	ft
m	meters	1.09	yards	yd
km	kilometers	0.621	miles	mi
SYMBOL	**WHEN YOU KNOW**	**MULTIPLY BY**	**TO FIND**	**SYMBOL**
AREA				
mm^2	square millimeters	0.0016	square inches	in^2
m^2	square meters	10.764	square feet	ft^2
m^2	square meters	1.195	square yards	yd^2
ha	hectares	2.47	acres	ac
km^2	square kilometers	0.386	square miles	mi^2
SYMBOL	**WHEN YOU KNOW**	**MULTIPLY BY**	**TO FIND**	**SYMBOL**
VOLUME				
mL	milliliters	0.034	fluid ounces	fl oz
L	liters	0.264	gallons	gal
m^3	cubic meters	35.314	cubic feet	ft^3
m^3	cubic meters	1.307	cubic yards	yd^3
SYMBOL	**WHEN YOU KNOW**	**MULTIPLY BY**	**TO FIND**	**SYMBOL**
MASS				
g	grams	0.035	ounces	oz
kg	kilograms	2.202	pounds	lb
Mg (or "t")	megagrams (or "metric ton")	1.103	short tons (2000 lb)	T
SYMBOL	**WHEN YOU KNOW**	**MULTIPLY BY**	**TO FIND**	**SYMBOL**
TEMPERATURE (exact degrees)				
^oC	Celsius	1.8C+32	Fahrenheit	^oF
SYMBOL	**WHEN YOU KNOW**	**MULTIPLY BY**	**TO FIND**	**SYMBOL**
ILLUMINATION				
lx	lux	0.0929	foot-candles	fc
cd/m^2	$candela/m^2$	0.2919	foot-Lamberts	fl
SYMBOL	**WHEN YOU KNOW**	**MULTIPLY BY**	**TO FIND**	**SYMBOL**
FORCE and PRESSURE or STRESS				
N	newtons	0.225	pound force	lbf
kPa	kilopascals	0.145	pound force per square inch	lbf/in^2

TECHNICAL REPORT DOCUMENTATION PAGE

1. Report No.	2. Government Accession No.	3. Recipient's Catalog No.

4. Title and Subtitle	5. Report Date
Reinforced Concrete Foundation Remote Monitoring	December 2018
	6. Performing Organization Code
7. Author(s)	8. Performing Organization Report No.
Brian Kopp, Juan Aceros, and Adel K. El Safty	
9. Performing Organization Name and Address	10. Work Unit No. (TRAIS)
University of North Florida 1 UNF Drive Jacksonville, FL 32224	11. Contract or Grant No. BDV34-977-09
12. Sponsoring Agency Name and Address	13. Type of Report and Period Covered
Florida Department of Transportation 605 Suwannee Street, MS 30 Tallahassee, FL 32399	Final Report April 2016 – December 2018
	14. Sponsoring Agency Code

15. Supplementary Notes

16. Abstract

This project investigated whether it is possible to remotely monitor reinforced concrete foundations for the purpose of corrosion detection. The focus of the project was on identifying and investigating a technology that could provide both the delivery of energy to, and communications with, embedded sensors without the additional installation of wiring. A radio frequency propagation technique that uses the reinforcing steel as a single wire transmission line was identified as the most appropriate candidate, and experiments were designed to determine its usefulness. Baseline experiments conducted at 2.4 GHz in air were successful and demonstrated that the designed interfacing couplers and impedance matching circuits were adequate. However, when the medium was changed to concrete, the attenuation was too severe to support either energy harvesting or communications. Reducing the operating frequency to 8 kHz and modifying the interface provided only slight improvement. Given the successful results when operated in air, it may be possible to transfer the technology to monitoring existing open-air steel structures such as bridges and towers. In addition, it may be possible to adapt the approach for use in reinforced concrete foundations that include concentric reinforcing steel structures that could be used as a two-wire circuit for both energy harvesting and communications.

17. Key Word	18. Distribution Statement
Steel reinforced concrete foundations, remote corrosion monitoring, energy harvesting, communications, single wire transmission line	No Restrictions.

19. Security Classif. (of this report)	20. Security Classif. (of this page)	21. No. of Pages	22. Price
Unclassified.	Unclassified.	57	

Form DOT F 1700.7 (8-72) Reproduction of completed page authorized

EXECUTIVE SUMMARY

This final report summarizes all research and results for the FDOT project entitled “Reinforced Concrete Foundation Remote Monitoring.” During this effort, the design and testing of a solution to provide energy harvesting from, and communications with, sensors encased in reinforced concrete structures, without additional wiring, was investigated. Following a literature search and analysis of the available technologies, a technique was selected to investigate with laboratory experimentation. The single wire transmission line technique, developed decades ago for use on overhead power lines was adapted for use in this project on reinforcing steel (rebar) embedded in concrete.

To investigate the utility of the single wire transmission line technique for use on rebar, a series of experiments were conducted that first validated the approach on rebar that was NOT encased in concrete. Instead, the rebar was first tested in an ambient air medium. After the validation tests were completed, testing in concrete was conducted.

To interface with the rebar in the most power-efficient way, special directional couplers were designed that focus the energy along the rebar in one direction. Their size is dependent on frequency, so to ensure the results would be transferrable to industry, a high frequency was used that kept the couplers physically small. By initially using 2.4 GHz, the associated couplers were constructed with a diameter of less than 10 centimeters when attached to the rebar. The couplers were constructed using advanced manufacturing techniques, including laser-cut copper components and computer-aided manufacturing for the plastic dielectric members.

The baseline testing in air verified that the rebar could function as a single wire transmission line and that the coupler design worked. However, when the experimentation moved to encasement of the rebar and couplers in concrete, the performance degraded significantly. The degradation in concrete was large enough to suggest that the use of a high frequency like 2.4 GHz may not support either communications or energy harvesting in reinforced concrete structures.

A second design approach was pursued that investigated the idea of a rebar single wire transmission line using a much lower radio frequency of 8 kHz. Since the use of directional couplers is not possible at such a low frequency, simplified mechanical connections were utilized. The second design was first validated in air and the results were acceptable. However, when placed in concrete, the performance was once again degraded significantly. Though the degradation was not as severe as when 2.4 GHz was used, it was still substantial enough to indicate that the rebar single wire transmission line approach faces challenges that may warrant consideration of other techniques for monitoring reinforced concrete structures. Several future areas of research were identified. including transferring the research to applications on existing steel structure monitoring (since the results in air were successful) and also consideration of the use of this research for reinforced concrete monitoring when there are concentric steel reinforcing structures present.

TABLE OF CONTENTS

LIST OF FIGURES

LIST OF TABLES

CHAPTER 1. INTRODUCTION

This Florida Department of Transportation (FDOT) research project investigated whether it was feasible to remotely monitor a reinforced concrete foundation for corrosion using embedded sensors without the addition of wiring infrastructure to connect to the remote monitoring sensors. The focus of the project was on identifying the most promising technology to deliver energy to and communicate with unwired remote sensors. There were several tasks necessary to complete the project. A literature search was conducted first, followed by an analysis of the candidate technologies, and then the final task was to perform laboratory experiments to investigate the most promising technology. In the original scope, an additional field experimentation task was planned, but due to the suboptimal laboratory results that were obtained, this task was cancelled.

The literature search covered two general topics. The first topic was corrosion monitoring and focused on identifying the most appropriate methods for remotely sensing corrosion. Instrumenting a remote corrosion sensor limited the appropriate methods to those that are repeatable without human intervention and only require low power. The second literature search topic was energy harvesting and communications. The literature regarding the second two issues is presented together because the mechanisms that enable the two processes are usually applicable to both energy delivery and communications. Discussions with the FDOT at the end of the literature search regarding corrosion determined that a simple embedded instrumentation sensor that implements a Wenner array and measures the resistivity and voltage in situ would be a useful first step in the remote sensing of corrosion.

Following the literature search, the second task analyzed the energy harvesting and communications technology options. None of the technologies currently being researched in the literature appeared appropriate for both energy harvesting and communications within a reinforced concrete foundation. However, an older technology, called single wire transmission line, was reviewed, analyzed, and determined to be the leading candidate technology for both energy delivery to, and communications with, concrete-embedded corrosion sensors.

Having determined the leading candidate technology, laboratory experiments were designed and conducted to evaluate whether single wire transmission line technology can support both energy harvesting and communications. The experimental design effort involved developing a coupler to inject and remove radio frequency energy on the reinforcing steel and also the design of experiments in both air and concrete. The experiments in air provided a baseline demonstration of how well the single wire transmission line couplers could be expected to work in concrete. When the results of the single wire transmission line experiments yielded poor results, a second design approach was attempted. This second approach used a lower frequency in an attempt to mitigate the attenuation that was encountered in the first design approach. For both the first and second design approach, tests with two or three couplers were conducted, as well as experiments on small cylindrical cages of reinforcing steel.

The report is organized according to the tasks that were executed. The literature search results are presented first in Chapter 2. The investigations into candidate energy harvesting and communication technologies are presented in Chapters 3 and 4, respectively. The single wire transmission line concept is introduced in Chapter 5. The first laboratory experiment design and test results are presented in Chapters 6 and 7, respectively. Similarly, the design and test results for the second approach are presented in Chapters 8 and 9.The conclusions and recommendations

on next steps are presented in Chapter 10, with references and an appendix at the end of the report.

CHAPTER 2. LITERATURE SEARCH

In this literature search 23 articles were found that are pertinent to this FDOT project on remote monitoring of reinforced concrete foundations. The FDOT Materials Lab worked with the UNF team, during task 1, to identify appropriate sensing parameters to use for this project. The parameters (potential and resistance) are indirect measures of corrosion and are relatively simple to implement. Six pertinent articles were found that address corrosion monitoring sensors. Two of these articles also discuss embedded sensors. There is evidence in these articles that affirm that the remote monitoring of corrosion using networked sensors is a useful methodology to consider.

In the bulk of the literature search, energy harvesting and power efficient communications were investigated to understand the state of the art and to consider alternatives for these two issues. The energy harvesting techniques are numerous but other than solar energy, the efficiency and reliability of the available schemes present a challenge within a concrete foundation. Also, since solar energy cannot be harvested from within a foundation a new approach to delivering energy to the remote sensors may have to be considered. The power-efficient communication methods investigated in the literature search were complementary to the energy harvesting articles. In fact, 14 of the 17 articles that discussed energy harvesting and communications, discussed both topics. Although many aspects of communications were discussed in the articles, including power efficient modulation and protocol designs, only two principal types of physical layer communication connectivity were discussed: traditional wireless and traditional wired networks.

A dominant feature of reinforced concrete foundations does not appear in the literature to have been leveraged yet for energy harvesting or communications. The reinforcement members are usually steel and their structure may have utility as a single wire transmission line (also referred to as a surface wave transmission line) for the transfer of both energy and communication signals.

The pertinent literature regarding corrosion monitoring includes six articles. All of them address monitoring corrosion related parameters using sensors. Song and Saraswathy [1] and Karwthick, Muralidharam, Sarasswathy, and Thangavel [2] also address some form of embedded sensing. Song and Saraswathy [1] presents a comprehensive survey of fifteen corrosion monitoring techniques. The discussions on potential and resistivity in this article are in line with the desires of the FDOT corrosion team at the Materials Lab in Gainesville who view these parameters as among both the most effective and easiest to investigate in this project. Song and Saraswathy also discuss embedded sensors, including an Embedded Corrosion Instrument (ECI) that measures potential and two types of resistivity, among five parameters (chloride ion concentration and temperature are the other two). The ECI sensor is networked using wire cables so power delivery and communications are trivial.

In Karwthick et al. [2], an embedded sensor that measures potential was monitored over a long-term, 24 month study to investigate the use of the sensor technology. The results suggest long term embedded sensing has merit. Krishan [3] discusses networking of sensors for monitoring corrosion. The approach gives credence to the idea of embedding multiple sensors in a reinforced concrete structure so that they can monitor the structure with a desired physical resolution.

Qiao, Sun, Hong, Liu, and Guan, [4], and Qiao, Sun, Hong, Qiu, and Ou [5] address a corrosion monitoring project that investigates several intriguing ideas. First, networked corrosion sensors are investigated that use a wireless network to communicate their data. In addition, in [5], power efficient operation using the actual corrosion process as a power source is described. The project discussed in [4] and [5] addresses reinforced concrete panels so embedding the sensors is not specifically addressed. However, the project acknowledges the idea that wireless sensors and power-efficient sensors are applicable to corrosion monitoring in reinforced concrete.

Khan, Khan, Nouman, Azhar, and Saleem [6] discuss the significant challenges of developing pH sensors for microelectromechanical systems. The first stage of the FDOT project will use potential and resistance measurements, however pH is a more direct form of corrosion monitoring (it indicates corrosion conditions directly) so as the technology improves, if power-efficient pH sensing in concrete becomes a reality, it would be a candidate parameter to include in a future remote monitoring system.

The majority of the pertinent literature addressing energy harvesting and communications focus on the two topics together. Only 3 articles [8, 10, 11] focus on energy harvesting alone. The article by Valenta and Durgin [8] discusses Radio Frequency (RF) energy harvesting principals and the requirements of a wireless power transfer system. The article also discusses how to characterize an energy harvesting circuit, and how to determine when maximum energy conversion efficiency has been achieved. A survey of RF energy harvesting technologies is also presented. In Raghunathan and Chou's article [10] the focus is on power management including charging profiles and node and network level power control. The last of the three energy-harvesting-only articles is by Chalasani and Conrad [11] and presents a survey of energy harvesting techniques, including some derivative techniques such as electrostatic energy harvesting using vibration dependent variable capacitors.

Only one article discusses energy harvesting, communication sensor networks, and corrosion. Sun, Qiao, and Xu [15] present the design of a framework for an energy harvesting sensor network to monitor corrosion in reinforced concrete. It is a continuation of the work presented in articles [4] and [5] with the inclusion of some additional information on networking.

Five pertinent articles survey energy harvesting techniques with a specific theme of addressing how it applies to communications. Vullers, Schaijk, Visser, Penders, and Van Hoof [7] discuss contemporary wireless sensor network applications in terms of power requirements and then introduce energy harvesting techniques including motion and vibration, temperature difference, photovoltaic, and wireless (non-conducted) radio frequency harvesting. Sudevalayam and Klkarni [12] present another survey of energy harvesting techniques. They also provide a comparison of the associated energy storage technologies. Networking considerations are also presented as well as some energy harvesting related comments on data collecting. In their survey of energy harvesting techniques, Ku, Li, Chen and Liu [13] provide information on energy use protocols and scheduling optimization. A significant amount of information is also provided on communication protocol design issues. Future areas of interest are also discussed. In the fourth energy harvesting survey article, Prasad, Devasenapathy, Rao, and Vazifehdan [14] provide information on communication protocol design issues including routing and media access control. In the last energy harvesting survey article Seah, Eu, and Tan [21] discuss the requirements for various aspects of a communications scheme for wireless sensor networks that

uses ambient energy harvesting. The communications aspects include routing, data delivery schemes, and network topology. Energy storage is also addressed.

There is a group of four articles that discuss energy harvesting and communications and focus on using wireless RF methods for both issues. Soyata, Copeland, and Heinzelman [9] discuss RF energy harvesting principles. They also address important topics including design tradeoffs, and provide an analysis of multi-mode operation where in the sensor system sleeps when not in use. Communication modulation types and their tradeoffs with harvesting are also considered. Zhang, Maunder, and Hanzo [17] present the state of the art in combined information and power transfer schemes using wireless RF techniques. They discuss the link between channel coding and modulation and the reliability of the system and also the use of multiple antennas in achieving practical systems. Radio interference is also discussed. In the third article discussing RF methods, Lu, Wang, Niyato, Kim, and Han [22] present a proposed step-by-step design approach to developing a wireless network that uses RF energy harvesting. Discussions and research on antenna design and receiver architecture are presented. Single hop multi-user schemes are discussed as well as multiple hop schemes. Protocols and multiple antenna schemes are also discussed. This article also includes an impressive energy harvesting technology comparison but the focus on RF was deemed more useful and so it was categorized with the other articles on RF methods and techniques. The last pertinent article that discusses RF methods is by Calhoun, Daly, Verma, Finchelstein, Wentzloff, Wang, Cho, and Chandrakasan [23]. In this article the authors focus on the architecture of a low power sensor node. The overall design is discussed as well as specifics regarding how to perform a fast Fourier transform and how to implement a low power analog-to-digital conversion circuit.

Three articles focus on optimization of energy harvesting and communication methods. Zhang and Lau [19] discuss the challenge of delivering information quickly but in a power efficient manner when there are multiple nodes and limited power. This article also discusses some higher-level communication protocol issues and analysis. It also proposes a solution that is power efficient and time sensitive. A second article discusses the importance of selecting the right communication medium access control protocol to ensure energy efficiency. In this article Ramezani and Pakravan [18] present a survey of MAC protocols and then provide the design aspects of a MAC protocol optimized for energy harvesting. Ozel, Tutuncuoglu, Ulukus, and Yener [20] discuss how to determine the communications capability for a specific energy harvesting profile. It relates energy arrival and energy expenditure to the communications channel performance.

One final article that was reviewed considers energy harvesting in combination with the use of a relatively new communications technique called cognitive radio. Mohjazi, Dianati, Karagiannidis, Muhaidat, and Al-Qutayri [16] present the issues associated with building cognitive radio networks using radio frequency energy harvesting.

CHAPTER 3. CANDIDATE ENERGY HARVESTING TECHNOLOGIES

Several of the energy harvesting articles reviewed in the literature search compared and contrasted the performance of various technologies. In the review by Vullers, Schaijk, Visser, Penders, and Van Hoof [7] technologies including photovoltaic, vibration, thermal, and radio frequency (RF) wireless energy harvesting are discussed. These technologies are also discussed in several other references on energy harvesting [22, 24, 25]. The information from all of these sources is combined in Table 1 to provide an opportunity to compare wireless energy harvesting technologies. The performance data in Table 1 can be easily compared across technologies because they are given as intensities, i.e., flux power densities per unit area.

For photovoltaic energy harvesting, data from the United States (U.S.) Department of Energy [24] were combined with industry research [25]. The data are for a typical Florida location and installation, and assumes the energy harvesting photovoltaic panel is a fixed flat panel perpendicular to the sun's arc at midday. The results are not unexpected as photovoltaic energy harvesting is a successful form of energy delivery.

Included in Table 1 are two industrial environmental energy harvesting techniques: vibration and thermal energy harvesting. While vibration energy harvesting can generate only modest amounts of energy, thermal energy harvesting, given sufficient heat, can generate energy levels similar to photovoltaic energy harvesting. Energy harvesting by vibration uses one of several electro-mechanical effects, e.g., the piezoelectric effect, to generate electrical energy due to vibratory motion. The vibrations can be man-made or environmental such as wind or ocean induced. Thermal energy harvesting leverages thermal differences between dissimilar metals to create a voltage and thus generate energy. The phenomenon is known as the Seebeck effect. The thermal differences can be man-made or due to environmental conditions such as solar heating.

Wireless RF energy harvesting is also included in Table 1. The available RF wireless energy was computed assuming far-field conditions and an isotropic omni-directional source radiating 1 watt of power in a vacuum or in dry air. An imaginary sphere of one-meter radius surrounding the source would have a surface area of 12.57 m^2, or 125,700 cm^2 (area = $4\pi r^2$ at r = 1 meter). At a distance of 1 meter from the source, a 1-square-centimeter area on this sphere receives only 8 μW of the 1-watt RF power transmitted from the source.

Efficiency values on the right of Table 1 help to explain how well each technology can harvest available energy. The key word is "available" energy. For technologies like photovoltaic energy harvesting, the source power can be quite high, assuming unobstructed outdoor exposure at a lower latitude is available. For a sensor embedded underground in a reinforced concrete foundation it would be necessary to wire the sensor to the photovoltaic source at the surface. This wiring is one of the vulnerabilities this research project is working to overcome. For the case of vibration energy harvesting, it may be possible to take advantage of the movement of a reinforced concrete bridge deck to harvest energy. However, most reinforced concrete foundations do not experience vibratory motion such as that of a bridge deck. Similarly, exposed reinforced concrete structures, such as bridge decks, may experience sufficient thermal variations from solar heating and ambient weather to produce useful energy. As with vibration though, subterranean concrete foundations do not regularly experience such thermal variations.

Table 1. Wireless Energy Harvesting Technologies

Technology	Source Power Density	Recovered Power Density	Maximum Efficiency
Outdoor Photovoltaic Fixed, Flat Panel in Tampa, Florida [24]	~5 kWh/m^2/day or ~20 mW/cm^2 averaged over a 24 Hour period or ~100 mW/cm^2 during the peak sun insolation period	~4mW/cm^2 averaged over a 24 hour period or ~20 mW/cm^2 during over the peak sun insolation period	20 % [25]
Industrial Vibration [7]	Mass and Displacement Dependent	< 100 μW/cm^2	N/A
Industrial Thermal [7]	100 mW/cm^2	1-10 mW/cm^2	1-10 %
Far-Field Radio Frequency Wireless (1 watt at a distance of 1 meter)	10 μW/cm^2	~5 μW/cm^2	50 % [22]

Using wireless RF energy harvesting as described above is challenging in dry air due to the spreading losses of propagation and even more so in an environment such as a reinforced concrete foundation. The attenuation of reinforced concrete has been measured by the National Institute of Standards and Technologies [26]. Pertinent results from the NIST report are summarized in Table 2 for a specimen of reinforced concrete that is 203 mm thick with a single-layer square grid of rebar embedded midway through the sample. The rebar square spacing was varied at either 70 mm or 140 mm. The attenuation data represents the additional loss the presence of the concrete sample creates relative to the expected loss in a vacuum or dry air test without the sample. The results show there is significant attenuation of RF energy within all tested types of unreinforced and reinforced concrete.

It is important to also note that the NIST tests were conducted on concrete samples in a laboratory environment. The samples were not buried in the ground where they can experience prolonged exposure to high moisture conditions and reactive soil conditions, both of which can change the attenuation conditions (conductivity) and the permittivity of the concrete. Water is an excellent absorber of RF energy. For frequencies above 1 MHz, RF attenuation losses increase with frequency for both fresh and salt water. At 1 gigahertz (GHz), for example, the attenuation loss in fresh water is approximately 50 dB per meter [27] and in sea water it is approximately 70 dB per meter [28].

The permittivity of concrete also increases with moisture content [29]. Permittivity is a critical factor in determining the ability of a material to support electrical energy transmission by RF propagation. When a concrete foundation experiences a higher moisture content, for example, within a submerged bridge pier, the concrete will exhibit a higher permittivity. A condition of

higher permittivity in effect, makes the concrete less able to support electrical energy transmission by RF propagation. The permittivity of concrete can also be impacted by the presence of salt in the concrete however the effect is minimal above approximately 1 GHz [30].

There are additional wireless energy harvesting techniques such as magnetic resonance coupling [22]; however, they are only useful over ranges of a few centimeters or at most a few meters, and, in the case of magnetic resonance coupling, require careful calibration procedures which would not be feasible given the presence of the reinforcing steel embedded in concrete and the variability of the associated construction process.

Table 2. NIST Wireless RF Attenuation Data For Concrete.

Frequency	Wavelength in Vacuum	Rebar Spacing	Attenuation Relative to Free-Space Loss
1 GHz	300 mm	140 mm	27 dB
2 GHz	150 mm	140 mm	31 dB
3 GHz	100 mm	140 mm	50 dB
1 GHz	300 mm	70 mm	30 dB
2 GHz	150 mm	70 mm	37 dB
3 GHz	100 mm	70 mm	53 dB

The review of the leading wireless energy harvesting techniques suggests that none of them is appropriate for use in a reinforced concrete foundation. The only wireless technology that may have applicability for use with concrete foundations is wireless RF propagation. However, at even a modest depth of a few meters the attenuation loss from propagation spreading combined with the losses associated with the concrete itself are so significant that the energy delivered would be trivial.

There may be an unconsidered technology that may provide a solution without resorting to the addition of wiring to deliver energy to sensors embedded in reinforced concrete. The science behind this technology is actually quite old, developed by Sommerfeld in 1899 [31]. Its use was first verified in 1956 by Goubau [32], who used it for communications on aerial conductors. The technology is called a single wire transmission line and the presence of reinforcing steel members in a reinforced concrete foundation may allow the technology to be adapted for energy harvesting.

CHAPTER 4. CANDIDATE COMMUNICATON TECHNOLOGIES

Task 1 explored the leading wireless communication techniques. Visual and infrared optical communications are not possible or practical for a sensor embedded in concrete. The leading wireless communication techniques all involve using RF communication. These techniques rely on the propagation of electromagnetic signals, usually by plane wave, through an interconnecting medium between a transmitter and receiver. This is the same propagation mechanism discussed above for energy harvesting via RF transmission.

As with energy harvesting, two significant issues for wireless RF communications in reinforced concrete are propagation spreading losses and the material effects on propagation of the concrete itself. Here, unlike for energy harvesting, weak signal propagation can potentially be used for wireless communications. For frequencies of interest, including up to several GHz, the spreading loss over the distances of interest (< 30 meters) are not significant for reliable communications. However, the conductivity and the dielectric effects (permittivity) of the concrete, in particular when saturated with water, are a concern and needs to be discussed in more detail.

If we consider concrete as a homogeneous medium (without cracks that would introduce additional challenging propagation boundary conditions) we can analyze the propagation effects of the concrete's conductivity and permittivity by considering the attenuation coefficient of an electromagnetic field in the medium. In general, the electric field of a time-varying electromagnetic signal can be expressed as a function of time t and position z using [33]

$$E = E_0 e^{j\omega t - \gamma z} \qquad (1)$$

where E_0 is the electric field magnitude, ω is the frequency in radians per second and γ is the propagation constant defined by

$$\gamma^2 = j\omega\mu_0\sigma - \omega^2\mu_0\varepsilon \qquad (2)$$

with material properties including magnetic permeability μ_0, conductivity σ, and permittivity ε. The material is assumed to be non-magnetic thus $\mu_0 = 4\pi * 10^{-7}$ Henries per meter is used. The propagation constant γ, expressed in Siemens per meter, is in general a complex quantity and can be expressed as

$$\gamma = \alpha + j\beta \qquad (3)$$

where α is the attenuation coefficient expressed in nepers per meter. The attenuation coefficient can be expressed in dB per meter with

$$\frac{dB}{m} = 8.686\frac{nepers}{m} \qquad (4)$$

The second coefficient, β, is the phase coefficient and is given in radians per meter. Substituting (3) into (1) yields

$$E = E_0 e^{-\alpha z} e^{j(\omega t - \beta z)} \qquad (5)$$

making it clear that the electric field magnitude is attenuated by the real exponential quantity $e^{-\alpha z}$, a function of both the position from the source and the attenuation coefficient. Solving (2) and (3) for α yields

$$\alpha = \omega \sqrt{\frac{\mu_0 \varepsilon}{2} \left[\sqrt{1 + \left(\frac{\sigma}{\omega \varepsilon} \right)^2} - 1 \right]} \qquad (6)$$

Therefore to evaluate the attenuation coefficient for concrete it is necessary to identify the conductivity, σ, and the permittivity, ε, at a desired frequency of propagation.

A particular frequency of interest for this research project is 2.4 GHz. The wavelength of this frequency in concrete is less than 10 cm. The reinforcing steel structure in typical concrete piers is made of steel members (rebar) up to approximately 2.5 cm in diameter which is less than a wavelength. In addition the spacing of the rebar is almost always greater than twice the wavelength. At a frequency of 2.4 GHz, these dimensions would tend to reduce the interaction between propagating electromagnetic waves (generally in TEM modes) and the reinforcing steel.

Therefore, extrapolating the results presented by Soutsos et al. in [29] for 2.4 GHz provides an estimated relative permittivity for typical homogeneous concrete of between approximately 4.5 and 7 and a conductivity of between approximately 0.01 and 0.25 Siemens per meter, with the respective limits associated with increasing moisture content from 0.2% (dry) to 12% (saturated). Inserting these estimates into equation (6) yields the attenuation coefficients given below in Table 3.

Table 3. Concrete attenuation coefficients at 2.4 GHz.

Water Content	Relative Permittivity	Conductivity (Siemens/meter)	Attenuation Coefficient (dB/meter)
Dry (0.20% Water, 99.8% Concrete)	4.5	0.01	7.71
Wet (5.50% Water, 94.5 % Concrete)	6.0	0.10	66.7
Saturated (12.0% Water, 88.0% Concrete)	7.0	0.25	153

These calculations suggest that there would be significant attenuation in all but the driest concrete structures, making communications at 2.4 GHz very difficult. In a low speed, 5 kilo-bit-per-second, communications system with a 100 milliwatt transmitter (or equivalently a 20 dBm transmitter), a typical industry-standard link receiver might have a minimum receiver sensitivity of -120 dBm at a relatively high 5% bit error rate. This suggests the link between the transmitter and the receiver must sustain no more than 140 dB of attenuation to function. Higher gain antennas can counteract the attenuation of the link but the cost is in the size of the antenna. If there is any moisture content in the concrete at all, the attenuation in a link beyond just a few meters would be difficult to overcome without using antennas whose sizes are measured in meters.

It should be noted that the data in Table 3 provide more optimistic results than the experimental results found by NIST [26]. However, the NIST experiments involved very closely spaced rebar which would likely be reflective to 2.4 GHz, and the experiments did not record the curing time or the water content of the test samples. In contrast, the data in Table 3 are based on Soutsos et al. [29], who conditioned their samples with either long duration air drying or submersion before accurately measuring moisture content. In addition, there was no rebar used by Soutsos, et. al. [29] in their samples.

To consider propagation at a lower frequency than 2.4 GHz, the data in Table 3 were recalculated using a much lower frequency of 70 MHz, and the results were mixed. While it appears propagation could be sustained at low to medium moisture levels, at higher moisture levels, the attenuation in the concrete is still prohibitive even for moderately large concrete structures (10 meters in length). In addition, the antenna structures at 70 MHz (wavelength in a vacuum of ~4 meters) are extremely large, making them impractical unless additional link loss (attenuation) is accommodated with a foundation-compatible undersized antenna design.

As with energy harvesting, it now appears that wireless communication techniques that involve the propagation of electromagnetic RF waves through the concrete medium will not provide a useful solution to communicating from embedded sensors. A “wireless” communication technique that may prove useful is the same one investigated above for energy harvesting. If a single wire transmission line can support energy transfer, it is likely that it can support communications.

It should be noted that an additional group of wireless communications techniques that may be considered in the future is acoustic and ultrasonic communications. There is very limited evidence in the literature of acoustic and ultrasonic communications being used with reinforced concrete. Recently, Scarton, Wilt, and Saulnier [34] demonstrated ultrasonic communications perpendicularly through a reinforced concrete column over a distance of 0.7 meters. However, there appears to be no research available regarding concrete-embedded acoustic and ultrasonic communications systems working at distances of multiple meters. Given the density and rigidity of a concrete foundation, it is suspected that the energy required to generate reliable communications with an embedded sensor would be significant and may be prohibitive for use in an energy-efficient communications system. Still, vibrating a concrete structure via acoustic and ultrasonic signaling is a testing technique used to analyze the health of a concrete structure, so it may be possible to augment this procedure to incorporate communications. As stated above, using this group of wireless communications techniques for embedded communications within concrete remains an open future area of research, and it is outside the scope of this project.

CHAPTER 5. SINGLE WIRE TRANSMISSION LINE CONCEPT

In a coaxial cable, transmitted wireless energy includes an electromagnetic field that typically propagates along the cable with both the electric and magnetic components of the field considered to be radiating between the center conductor of the cable to the outer conductor, perpendicular to the direction of propagation along the cable. The electric and magnetic fields are also perpendicular to each other, existing in a plane that is perpendicular to the direction of propagation[1]. The electric field vector is considered to be linear and radiating outward from the center conductor. However, the magnetic field is circular, creating rings of varying field strength around the center conductor. Together in this configuration the two fields are called a Transverse Electric Magnetic (TEM) propagation wave. Elmore [35] and Goubau [36] both theorized that if the coaxial cable outer diameter is increased without bound, the electric field component of the TEM wave will eventually collapse and all that will remain is a Transverse Magnetic (TM) wave that propagates along the former center conductor. The TM wave will remain close to the center conductor and interact only with the surrounding medium that is in the immediate circumference around the center conductor. By designing a coupling mechanism that allows for a coaxial interface to transition into a single wire transmission line, and then back again to a coaxial interface at the far end of the link, a complete transmission system is created.

Both Elmore [35] and Goubau [36] have demonstrated the concept in an air medium. Sharp and Goubau [37] demonstrated a single wire transmission system that experienced less than 50% power loss at a 130-foot distance for a transmission frequency as high as 2.4 GHz. Elmore [35] developed a version of the single wire transmission system that can be manufactured and installed on overhead power lines. His results suggest in a practical environment only 80% of the power will be lost over a 60-foot distance. Such losses are easily accommodated by todays energy harvesting and communications circuit technologies.

Both the Elmore and the Goubau approach use a similar shape for the launch mechanism. The shape has two sections, a cylindrical section for propagating a coaxial TEM mode and also a conical expanding section to launch the TM mode onto the single wire. The conical expanding section matches the diameter of the cylindrical section at its narrow end as shown in the concept drawing in Figure 1. In addition, the cylindrical section includes a tap to inject and extract power or communication signals. A coaxial connector is connected to the single wire transmission line at a distance of a quarter wavelength from the end plate of the cylindrical section. The end plate presents a short-circuit between the single wire transmission line and the outer conductor of the coupler.

The Elmore and Goubau solutions assumed that the single wire transmission line is intended to be used in an air medium. Their coupler construction techniques included an internal air medium for the dielectric between the single wire transmission line and the outer conductor as well. This project investigated the use of a single wire transmission line embedded in concrete. The dielectric properties of concrete and air are different. To compensate for the dielectric difference, the embedded version of the couplers were constructed with a dielectric material that substituted for concrete, ensuring minimal impacts to the boundary conditions where the coupler and concrete meet. The material chosen was Polyvinyl Chloride (PVC) plastic. It should be noted

[1] Elmore [35] theorizes that there is a second field present in the coaxial cable at all times that consists chiefly of a perpendicular magnetic field.

that the speed of light is slower in higher permittivity materials like PVC and this decreases the wavelength of the frequency being transmitted[2]. The decreased wavelength was accommodated in the coupler designs.

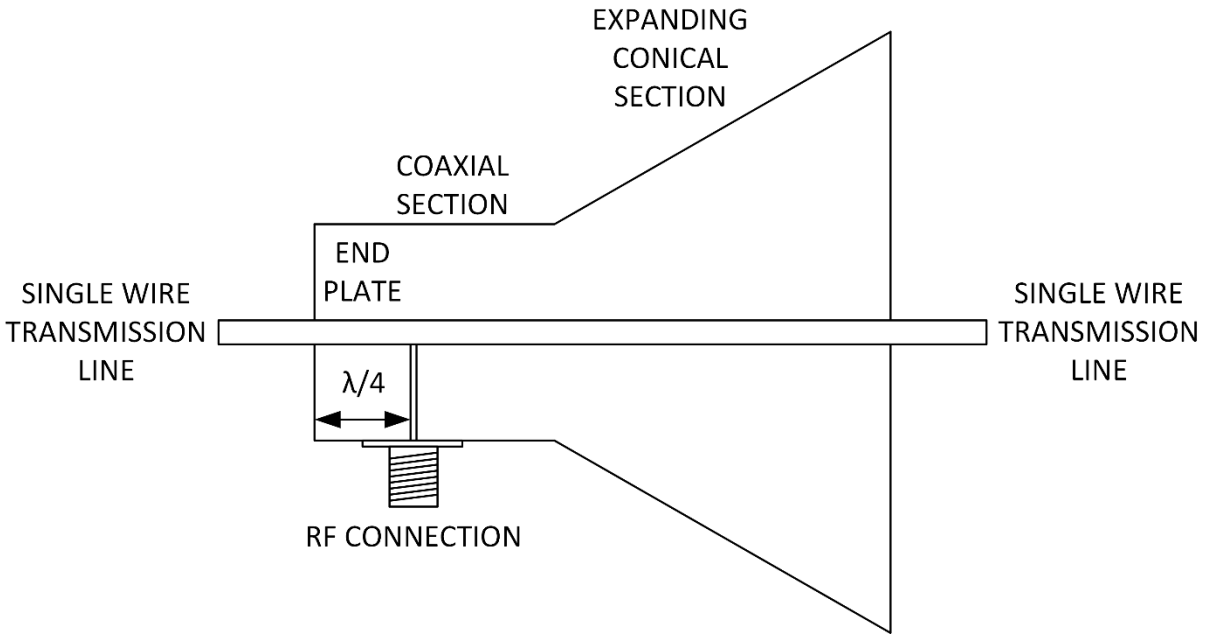

Figure 1. Concept drawing of single wire transmission line coupler.

According to Goubau [38], if the surface of the center conductor is roughened or coated with a dielectric, the radial distance away from the rebar in which the TM mode wave will propagate will be reduced significantly. This is an advantage since it keeps energy from radiating outward and being lost and it minimizes absorption in the medium around the single wire transmission line. It was theorized that the standard ridging around the circumference and all along the length of rebar, combined with any surface rust will have this desired effect on propagation.

First Single Wire Transmission Line Solution

The first attempt to develop a single wire transmission line solution involved the development of a coupler similar to that of Elmore and Goubau. The operational frequency that was chosen was 2.4 GHz. This frequency has several advantages. It was investigated in the work by Sharp and Goubau [37] so there is precedence for its use. It has a small wavelength of 12.5 centimeters (cm) in air. In concrete with a high relative permittivity of 10 the wavelength would be 4 cm. Even with a lower relative permittivity of 3, the wavelength is still smaller at 7.2 cm. This means the coupler designs for use in concrete will be small. This is an important consideration in reinforced concrete structures where the reinforcing steel is often times only a few centimeters below the surface of the concrete. Using this small wavelength also simplifies test set up

[2] The wavelength is calculated using $\lambda = \frac{c}{f\sqrt{\varepsilon_r}}$ where c is the speed of light, f is frequency, and ε_r is relative permittivity.

concerns about interference since any radiated energy attenuates quickly. In addition, the frequency range at 2.4 GHz is associated with unlicensed spectrum and therefore there is less concern about the single wire transmission system causing interference.

The initial experiments were conducted in air to baseline the design before moving to embedded couplers. Point-to-point coupler set ups along a straight piece of reinforcing steel or “rebar” were tested as were point-to-point coupler set-ups where one coupler was on a perpendicular piece of rebar that was mechanically connected to another piece of rebar where the second coupler was.

Second Single Wire Transmission Line Solution

The testing of the first solution did not yield acceptable results at 2.4 GHz when embedded in concrete. It was theorized that either water content in the concrete or the concrete itself was attenuating the 2.4 GHz signal and that a different signal of a few thousand kilo-Hertz (kHz) may propagate along the single wire transmission line. Specifically, 8 kHz was considered. Since the wave length of 8 kHz is 37.5 kilometers the coupler approach used for the first design was not appropriate. Instead, simple mechanical connections were made to the rebar. Again, testing was conducted first in air and then in concrete using both point-to-point straight and point-to-point perpendicular coupler connections.

Eight experiments are reported on in this task report. Six experiments were conducted on the first design approach and two experiments were conducted on the second design approach. Results are presented in both tabular and graphical form. Experiment schematic drawings and set-up photographs are also presented. The task report closes with concluding remarks on the test results.

CHAPTER 6. SINGLE WIRE TRANSMISSION LINE DESIGN 1

Implementing a solution for this project based on the concept of the single wire transmission line requires that electromagnetic energy to be coupled to the reinforcing steel in the concrete. For the first design approach a coupler was built using copper sheeting to form the outer conductor. As discussed above, PVC plastic was used as the dielectric and also the support for the outer conductor. The dimensions of the constructed coupler are shown in Figure 2 and were developed within the constraints presented in Elmore [35], Goubau, [36, 38], and Sharp and Goubau [37].

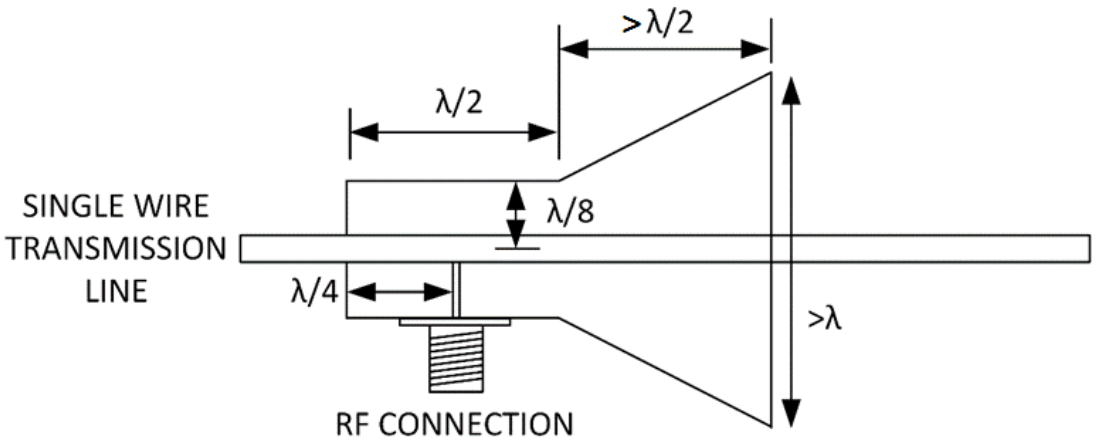

Figure 2. Coupler Dimensions.

The coupler prototype is shown in Figure 3. The gray PVC plastic was milled from a solid cylinder and then drilled for the coaxial tap. The copper sheeting was laser cut and then glued to the PVC. Copper tape was used to secure the assembly and ensure conductivity of the outer conductor. In Figure 4, an installed coupler is shown. The coaxial tap was achieved using a brass standoff soldered to the SMA coaxial connector center pin. The number 5 rebar (5/8” diameter) was drilled and countersunk for a Metric 2 (M2) stainless steel machine screw that passed through the rebar and screwed into the standoff. The tap components are shown in Figures 5 and 6. The screw provided the conductivity between the rebar and the coaxial tap and also added strength to the entire coupler assembly.

Figure 3. Coupler Prototypes.

Figure 4. Installed Coupler.

Figure 5. Standoff soldered to the coaxial tap SMA connector.

Figure 6. Machine screw through drilled hole in rebar.

There is a small Printed Circuit Board (PCB) attached to the coaxial tap in Figure 4. The PCB is there to provide the necessary impedance matching, ensuring maximum power transfer is achieved when the coupler is attached to the rebar. The impedance of the coupler alone was determined using a 2-port Vector Network Analyzer (VNA). The impedance was complex with real part varying between 30 and 60 Ohms and an imaginary part (reactance) varying between 90 and 130 Ohms. An impedance matching circuit was designed that matched a coupler impedance of 45+j110 Ohms to 50 Ohms. The circuit is a single stage Pi network and is shown in the simulation schematic-capture screen shot in Figure 7.

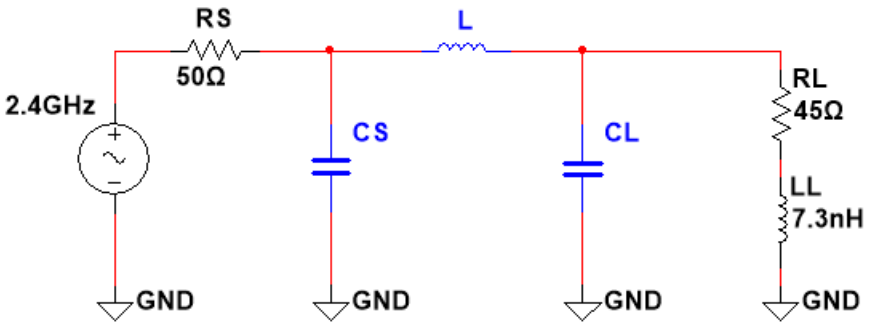

Figure 7. Impedance matching circuit for a 2.4 GHz coupler.

The impedance for the matching network can be solved using

$$Z_{in} = \left(\left((R_L + jX_L) \parallel \frac{1}{j\omega C_L} \right) + j\omega L \right) \parallel \frac{1}{j\omega C_S} \qquad (1).$$

The component values for CS, CL, and L that solve (1) for a $Z_{in} = 50$ Ohms assuming a modest circuit quality factor of three[3] is shown in Table 4. It should be noted that due to stray capacitance the final capacitor values were adjusted and are shown in parenthesis in Table 4.

Table 4. Component values for the 2.4 GHz matching network.

Component	CS	L	CL
Value	3.98 pF(5.0 pF)	3.6 nH	2.18 pF (1.4 pF)

The printed circuit board for the impedance matching circuit was manufactured using 0603 size surface mount components and its computer aided design is shown in Figure 8. The two sets of five large holes accommodate input and output coaxial connectors.

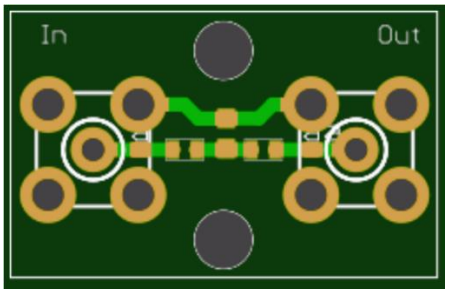

Figure 8. Computer aided design of impedance matching PCB.

[3] Quality factor in a filter or matching network is typically the ratio of the desired frequency of operation divided by the bandwidth of operation. In general, as the Q factor increases so does the required number of circuit stages.

CHAPTER 7. SINGLE WIRE TRANSMISSION LINE DESIGN 1 TESTING

Performance tests on segments of rebar were conducted first in air and then in concrete. The tests in air were baseline tests conducted to investigate how the couplers and rebar, working together, perform as a single wire transmission system similar to those developed by Elmore [35], Goubau, [36, 38], and Sharp and Goubau [37]. Afterwards tests in concrete were conducted.

Tests were conducted using a pair of couplers and also using three couplers. In the two coupler tests the couplers were arranged inline facing each other in a linear arrangement on a common piece of rebar. In the three coupler tests the third coupler was attached to a small piece of rebar that was mechanically secured to the inline piece of rebar used by the other two couplers. Tests were conducted with both a VNA and a 2.4 GHz source with a spectrum analyzer receiver. The VNA permitted the capture of network S parameters as well as impedance information about the couplers.

The first experiment investigated two couplers on a single piece of rebar. The couplers were connected to a VNA as shown in Figure 9. The arrangement of the actual couplers for experiment 1 is shown in Figure 10. The spacing of the couplers is 110.5 cm which is approximately nine wavelengths. This distance was chosen after investigating the electric and magnetic field strength near the rebar. This field strength research is included in Appendix 1.

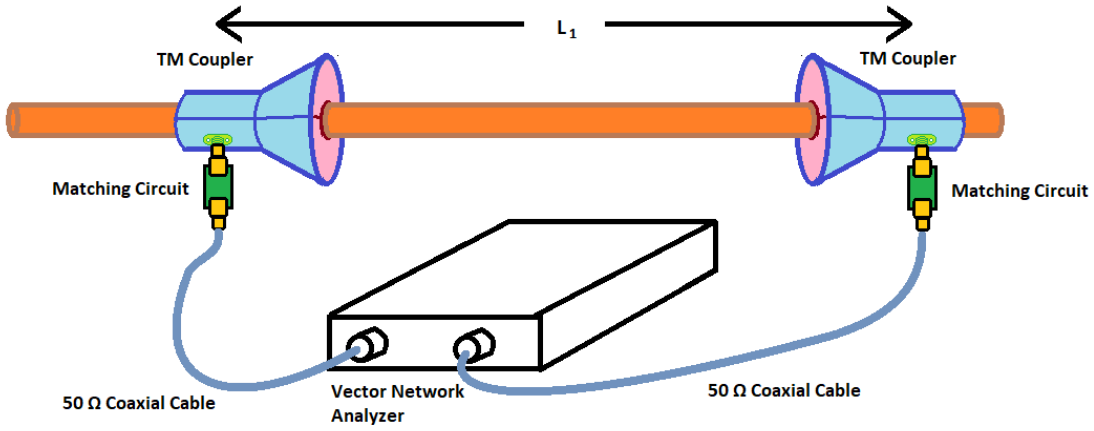

Figure 9. Experiment 1 schematic with two couplers in air and a VNA.

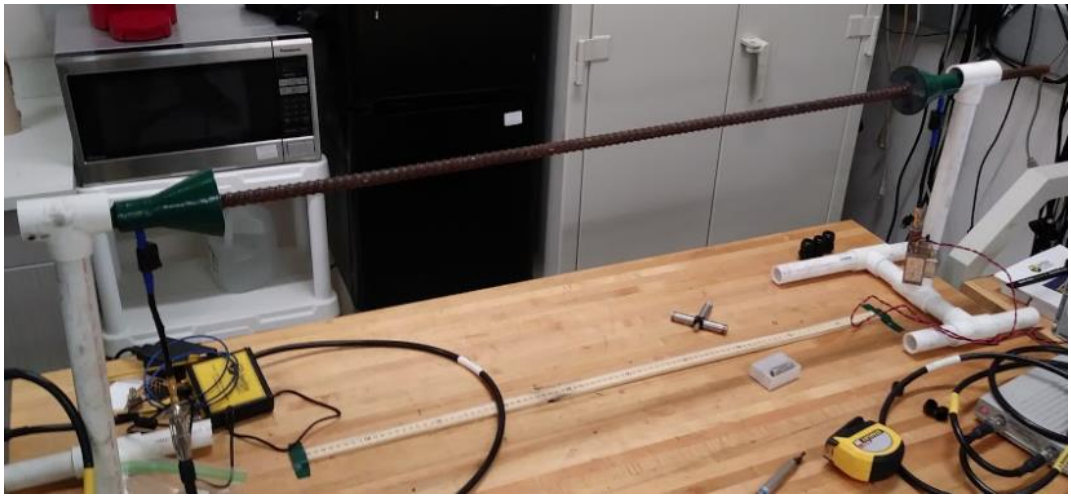

Figure 10. Experiment 1 set-up.

The matching circuits from two couplers were connected to the ports on a two-port VNA. The VNA recorded both log-magnitude and smith charts of the S-parameters for the two-coupler rebar system. A plot of the data referenced to port 1 is shown with the combined Smith chart and log plot in Figure 11. A similar plot of the data referenced to port 2 is shown in Figure 12. The plot data can be combined into a common table and displayed together as is shown in Table 5. The impedance looking into each coupler's matching circuit is given as Z_{in}. The S11 and S22 parameters relate how much of the VNAs transmitted power is reflected back toward the VNA and not transmitted at that port. The numbers are low (S11 = -19.7 dB) and indicate that only a small amount of power is prevented from being transmitted through the coupler. The S21 parameter conveys the power transmitted from port 1 that arrives at port 2. It is considered an insertion loss characteristic for the single wire transmission system. The S21 insertion loss is -15.6 dB, indicating that some power has radiated from the rebar but that a fraction of the transmitted power (2.7%) has been received by the other port. Similarly, the S12 parameter conveys the power transmitted from port 2 that arrives at port 1. The level of -14.4 dB indicates that 3.6% of the power has been received. While these insertion loss levels of receive power may seem low, they are not, compared to free space loss, which by comparison would deliver only 0.05% of the transmitted power (32.8dB of loss). This suggests that the single wire transmission line technique applied to reinforcing steel in air propagates better than traditional wireless free space transmissions by a factor of about 70.

Table 5. Experiment 1 VNA results for a two-coupler set-up in air.

Port 1 Z_{in} (Ω)	**S11 (dB)**	**S21 (dB)**	**Port 2 Z_{in} (Ω)**	**S22 (dB)**	**S12 (dB)**
40.6 + j1.06	-19.7	-15.6	51.6 - j12.6	-18.1	-14.4

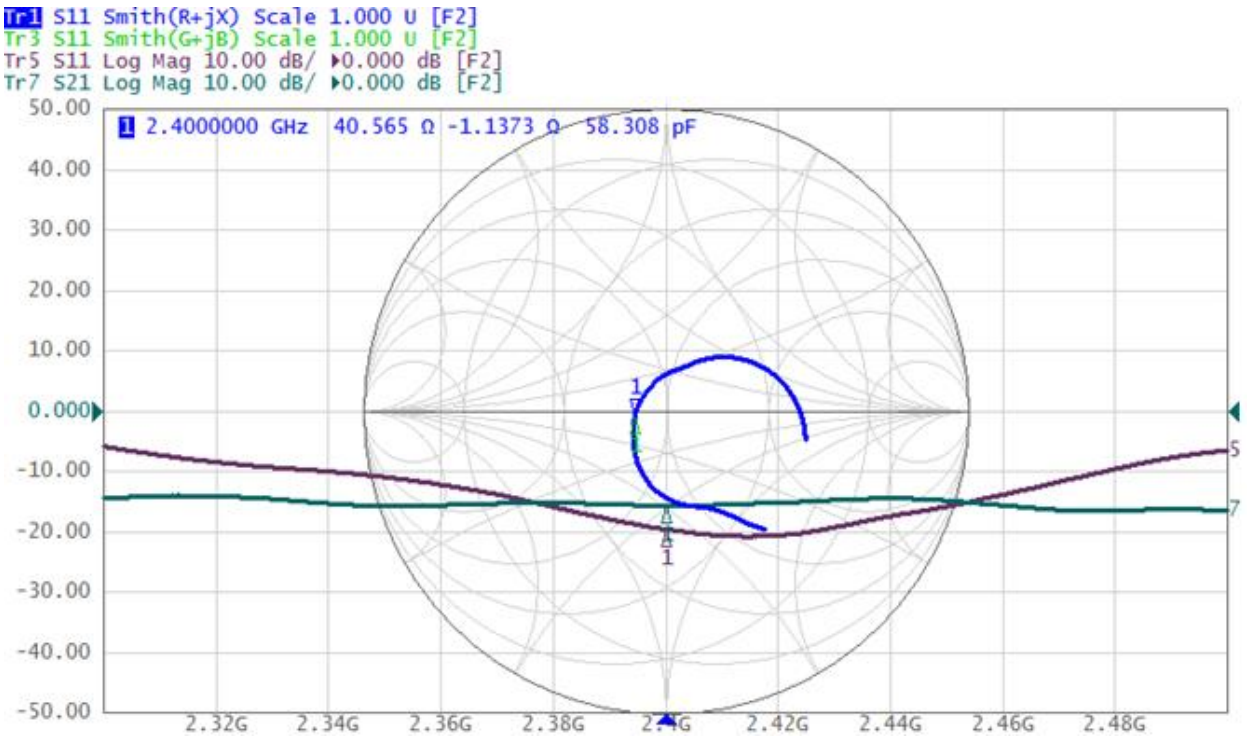

Figure 11. Port 1 S-parameters for a two-coupler system in air.

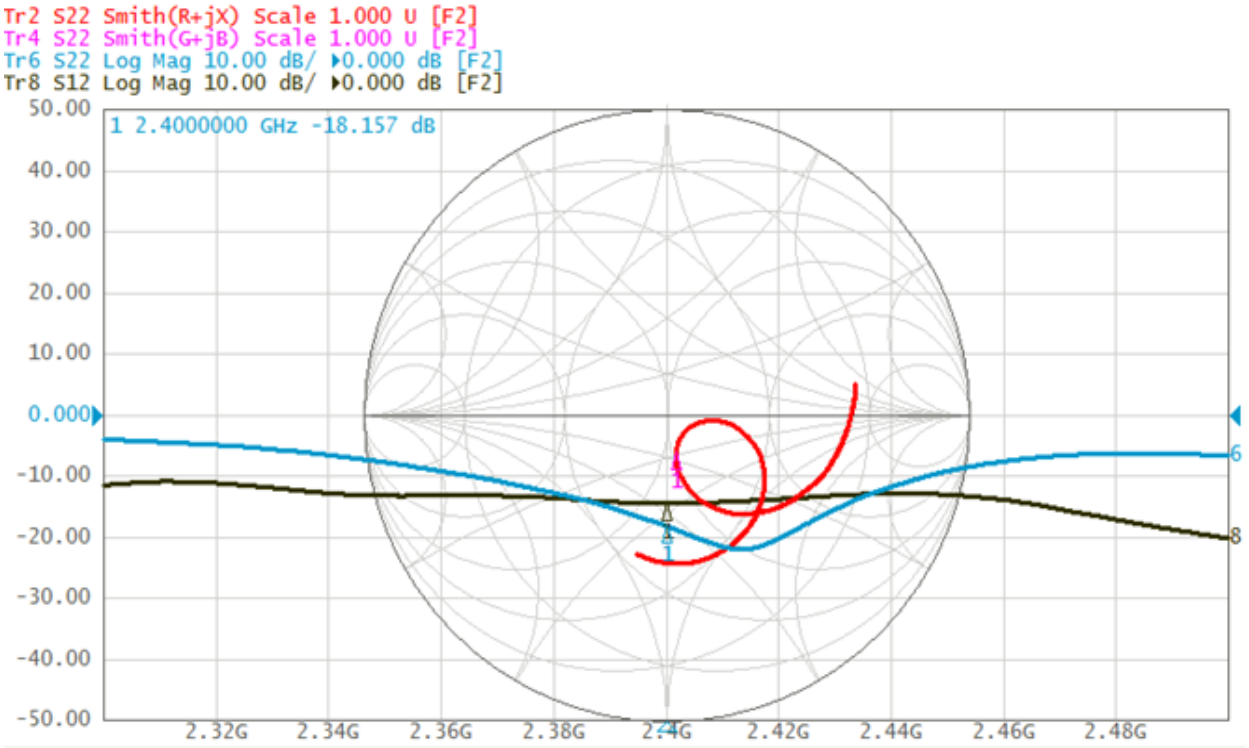

Figure 12 Port 2 S-parameters for a two-coupler system in air.

In experiment 2, the two-coupler test in air was repeated with a stable 2.4 GHz RF source known as an Oven Controlled Crystal Oscillator or OCXO, acting as a one -way transmitter attached to

the former port 1 coupler, and a spectrum analyzer acting as a receiver attached to the former port 2 coupler. The schematic for experiment 2 is shown in Figure 13. With a transmitted power of 19.8 dBm and a received power of 5 dBm, the insertion loss (equivalent to the S21 parameter from Experiment 1) was 14.8 dB. This is similar to the 15.6 dB measured by the VNA and acted as a verification tool using an actual RF transmitter source. The receive end of the experiment 2 test set-up is shown in Figure 14.

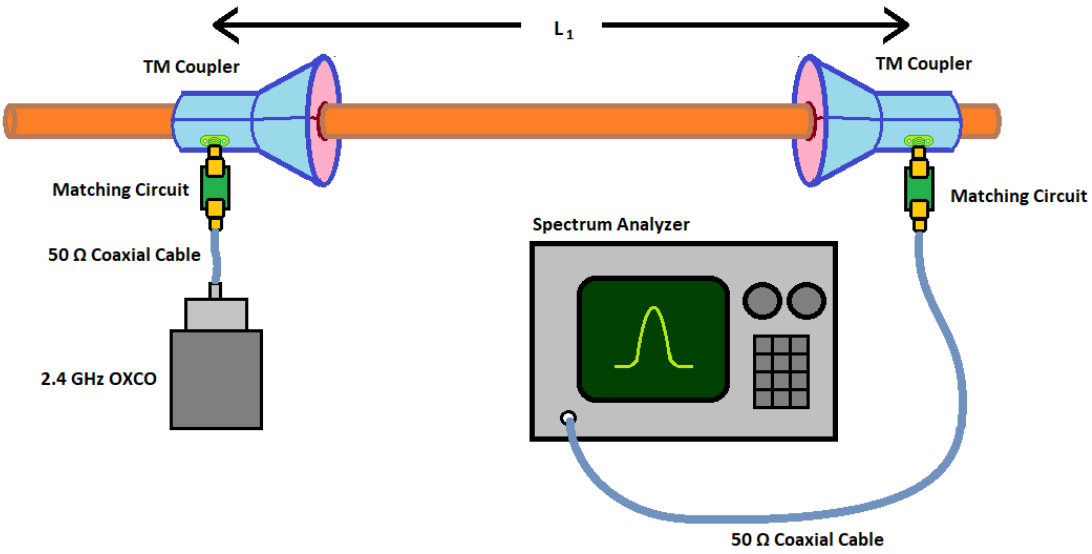

Figure 13. Experiment 2 schematic.

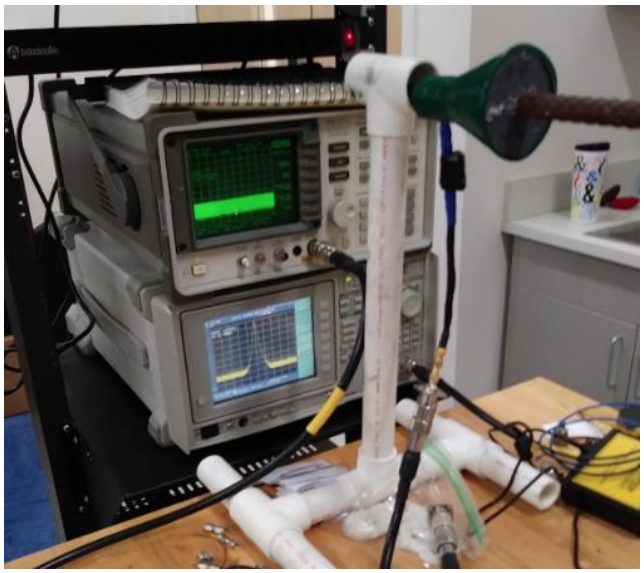

Figure 14. Experiment 2 receiver end set-up.

After completing the two-coupler experiments in air a third coupler was added to investigate perpendicular coupling on a typical rebar structure. The configuration for experiment 3 is shown

in Figure 15. The experiment 3 set-up is shown in Figure 16. The S parameters were measured using the configurations shown in Figure 17 with distances L1 = 110.5 cm and L2 = 61.6 cm. The perpendicular coupler was placed close to the inline rebar to consider only the impact of being at a perpendicular orientation and no other propagation effects. In other words, the perpendicular coupler is still within close proximity of the inline rebar and should experience the same field intensity as an inline coupler. A bracket attachment was used for the perpendicular coupler that allowed the coupler to be placed at any location along the inline rebar. When conducting the 2 port VNA tests between a pair of couplers in the three-coupler configuration, the matching circuit on the unused coupler was terminated into 50 Ohms.

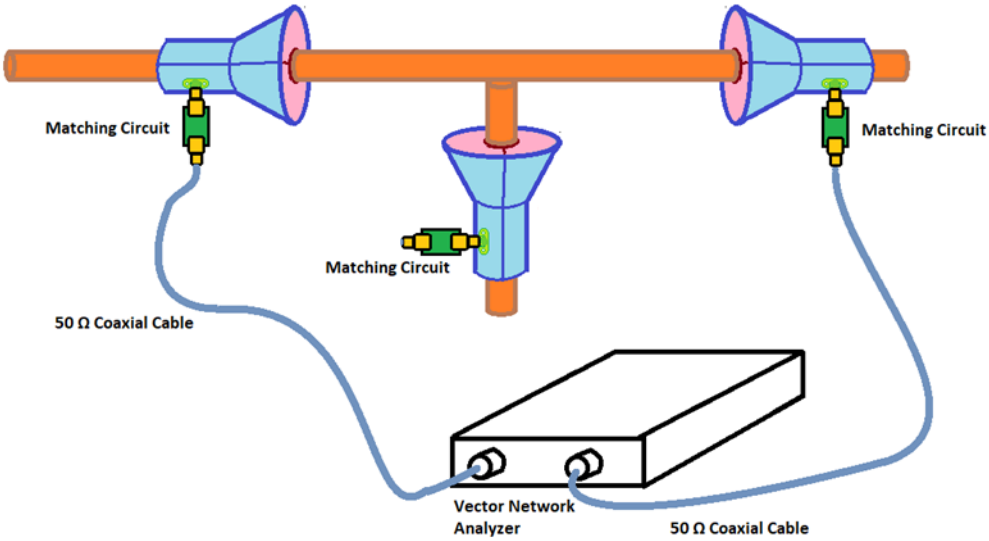

Figure 15. Experiment 3 schematic.

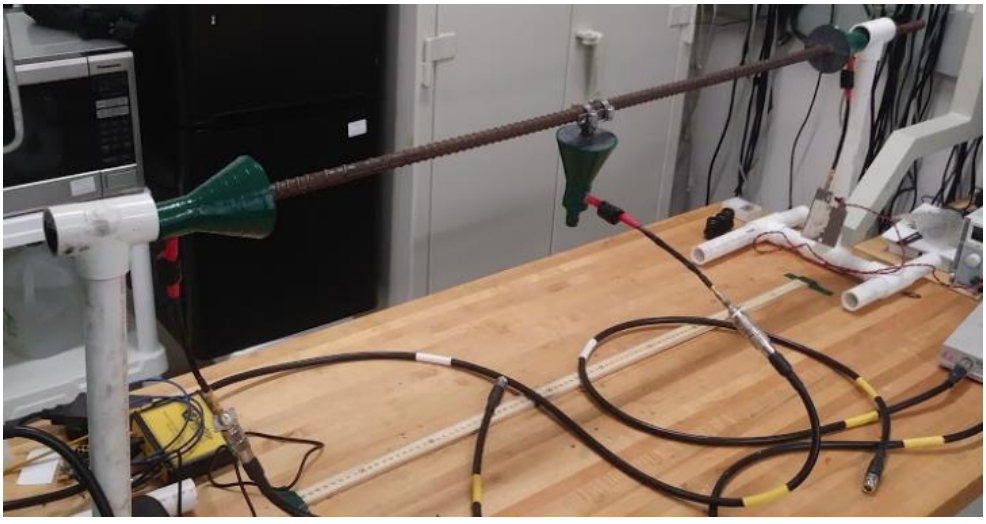

Figure 16. Experiment 3 set-up.

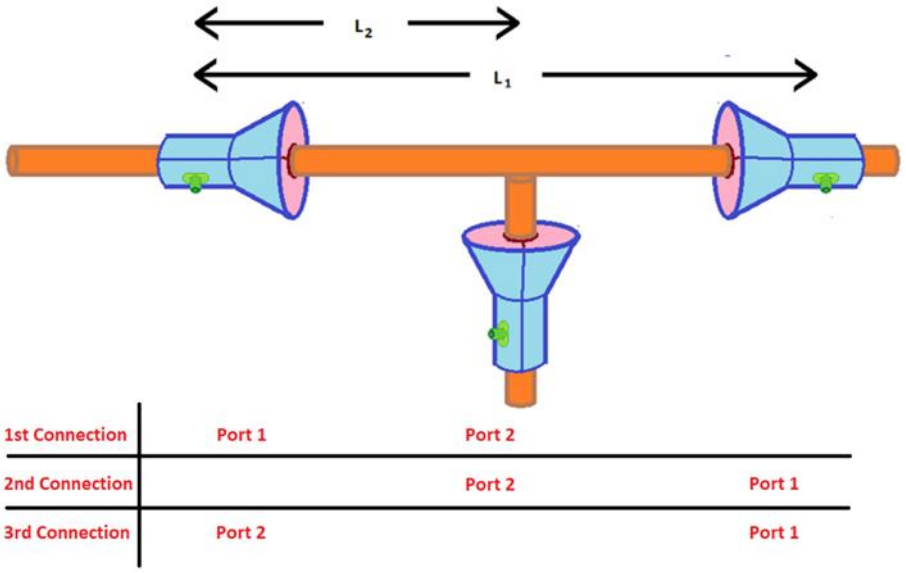

Figure 17. Experiment 3 S-parameter configuration.

The results for experiment 3 are shown in Table 6. Connection 3 of the experiment 3 results is essentially a baseline that matches the experiment 1 results. The connection 1 and connection 2 results indicate the perpendicular coupler has approximately 10 dB more insertion loss than the inline couplers which means that perpendicular coupler must contend with more loss than an inline connection. The additional loss is not an insurmountable loss insofar as communications or energy harvesting are concerned.

Table 6. Experiment 3 results.

Connection	**Port 1 Z_{in} (Ω)**	**S11 (dB)**	**S21 (dB)**	**Port 2 Z_{in} (Ω)**	**S22 (dB)**	**S12 (dB)**
1st	60.6 + j22.5	-13.1	-25.7	44.1 + j32.2	-9.34	-25.7
2nd	38.4 + j3.4	-17.3	-25.2	47.1 + j30.7	-10.3	-22.8
3rd	37.0 + j3.8	-16.1	-16.1	63.7 + j19.6	-13.6	-13.6

The three-coupler configuration in air was also analyzed using the same 2.4 GHz oscillator in the fourth experiment. Two spectrum analyzers were used to receive the transmitted 2.4 GHz signal on two couplers simultaneously. The schematic for experiment 4 is shown in Figure 18. The L1 distance remained 110.5 cm while the L2 distance was varied. The two receive couplers, one inline and one perpendicular are shown with their spectrum analyzers in Figure 19.

The results for the inline coupler insertion loss were the same as with the VNA. There was an average of 15 dB insertion loss in experiment 4. There was a minor variation of approximately 1

dB for the inline insertion loss when the location of the perpendicular coupler was changed. The results for the perpendicular coupler as it was moved along the inline rebar appear to follow the oscillating results from the electro-magnetic field strength tests discussed in Appendix 1. Both the inline and perpendicular coupler insertion loss results are shown graphically in Figure 20. The results for the perpendicular coupler are sensitive to position. A 5 dB variation in insertion loss was associated with the position of the perpendicular coupler. The average insertion loss for the perpendicular coupler was approximately 24 dB, which is consistent with the experiment 3 results.

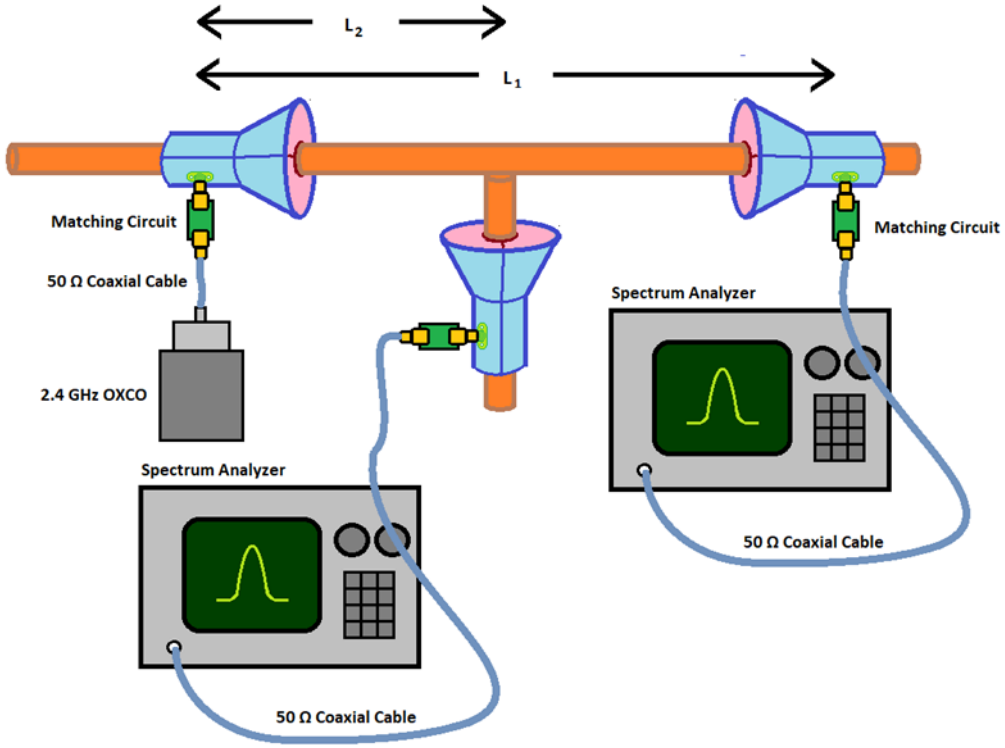

Figure 18. Experiment 4 schematic.

Figure 19. Experiment 4 inline and perpendicular receive couplers.

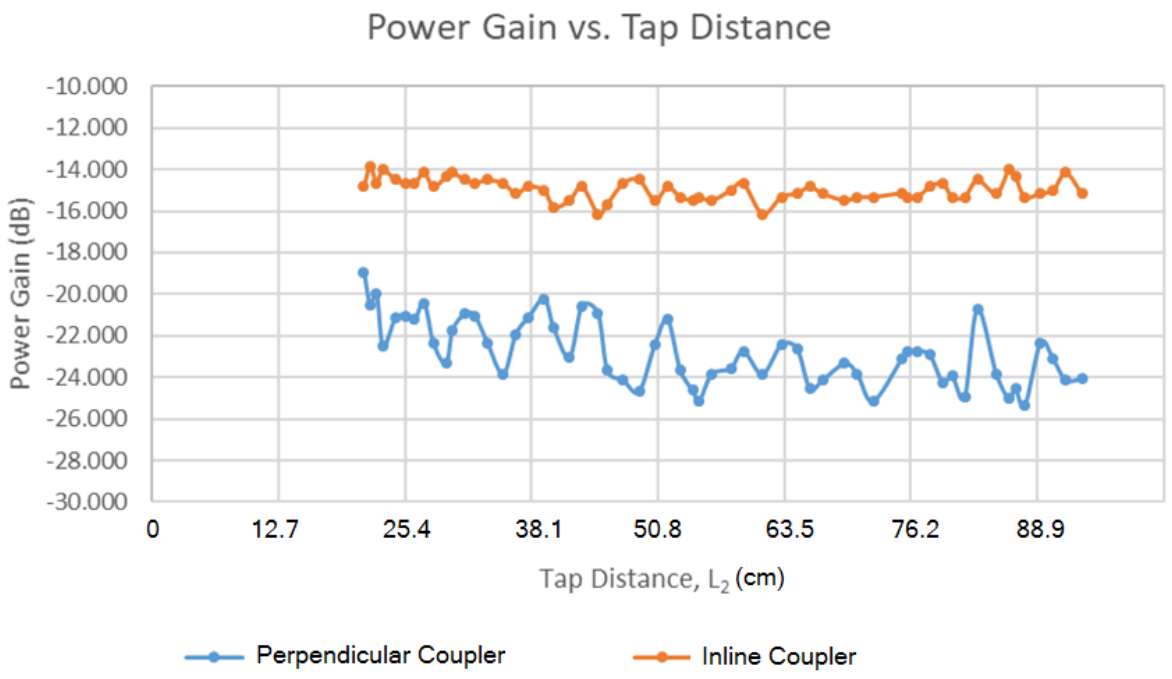

Figure 20. Experiment 4 results.

After the four experiments with the couplers installed on segments of rebar in air were completed, experiments were conducted with the couplers installed on segments of rebar that were encased in concrete. The concrete used in the experiments was mixed by hand using weight ratios of 1 part water, 2.5 parts cement, 2.75 parts sand, and 5 parts course aggregate. To fill a standard 12-inch diameter, 48-inch long, round cardboard concrete form required approximately 450 pounds of concrete. Holes were drilled in the side of the form to pass coaxial coupler cables out of the concrete.

Experiment 5 investigated two couplers installed inline on a segment of rebar encased in concrete. The schematic for the experiment is shown in Figure 21. The concrete in the experiment was allowed to cure for 12 days before the measurements presented here were taken. Figure 22 shows one of the concrete structures used for these experiments. A VNA test at 2.4 GHz with a bandwidth of 20 MHz was conducted. The coupler at the top of the concrete encased rebar was connected to port 1 of the VNA and the bottom coupler was connected to port 2 of the VNA.

Figure 23 shows the port 1 VNA results at 2.4 GHz for experiment 5. The port 2 results are shown in Figure 24. The S-parameters both indicate very good return loss performance but also very poor insertion loss performance. The S12 and S21 insertion loss parameters show that there is at least 90 dB of insertion loss. In fact, the insertion loss is so large, the VNA can not register any transmission of energy through the concrete. The low S11 and S22 return loss performance suggest the energy is leaving the couplers and entering the concrete. However, the extremely low S12 and S21 insertion loss performance suggest the energy is likely being absorbed by the concrete surrounding the rebar. The impedance matching networks appear to be functioning well since the impedance of both ports is approximately 46.5 + j4.0 Ohms which is close to 50 Ohms.

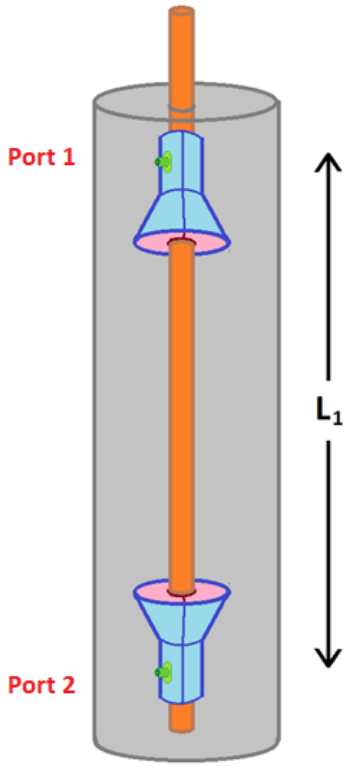

Figure 21. Experiment 5 schematic.

Figure 22. Example rebar-in-concrete experimental set-up.

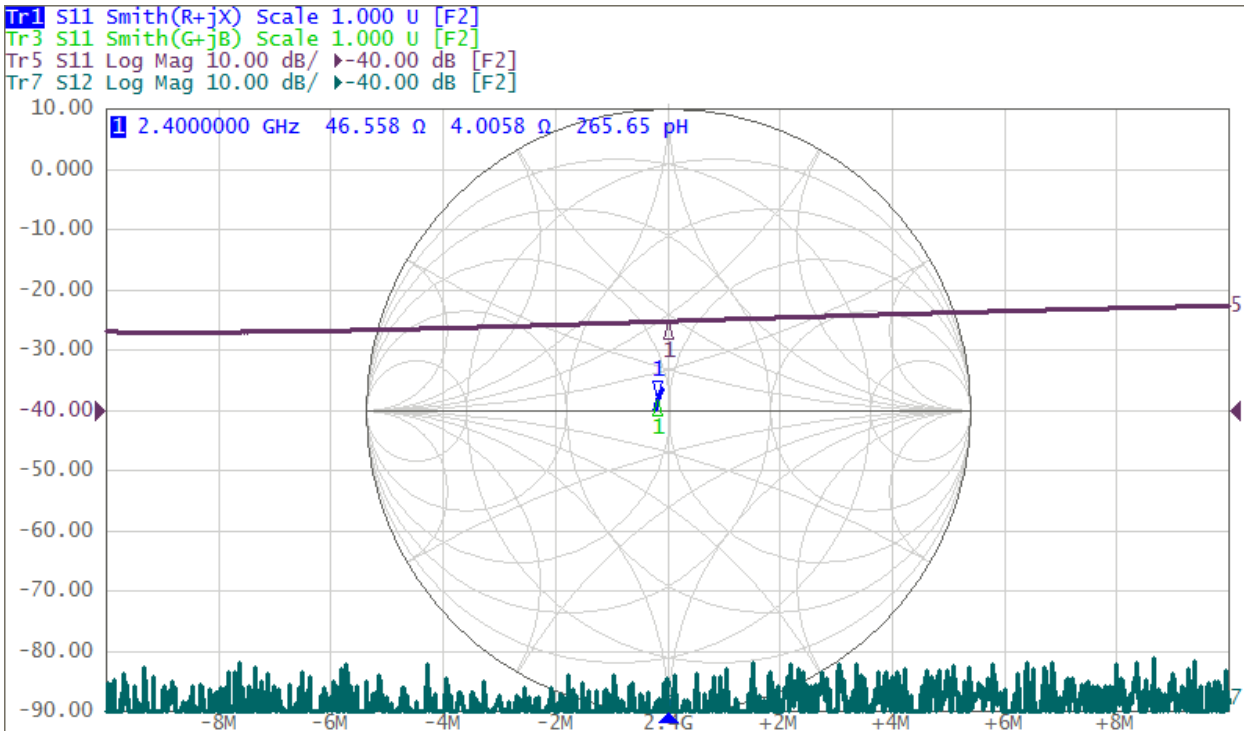

Figure 23. Experiment 5 port 1 results at 2.4 GHz.

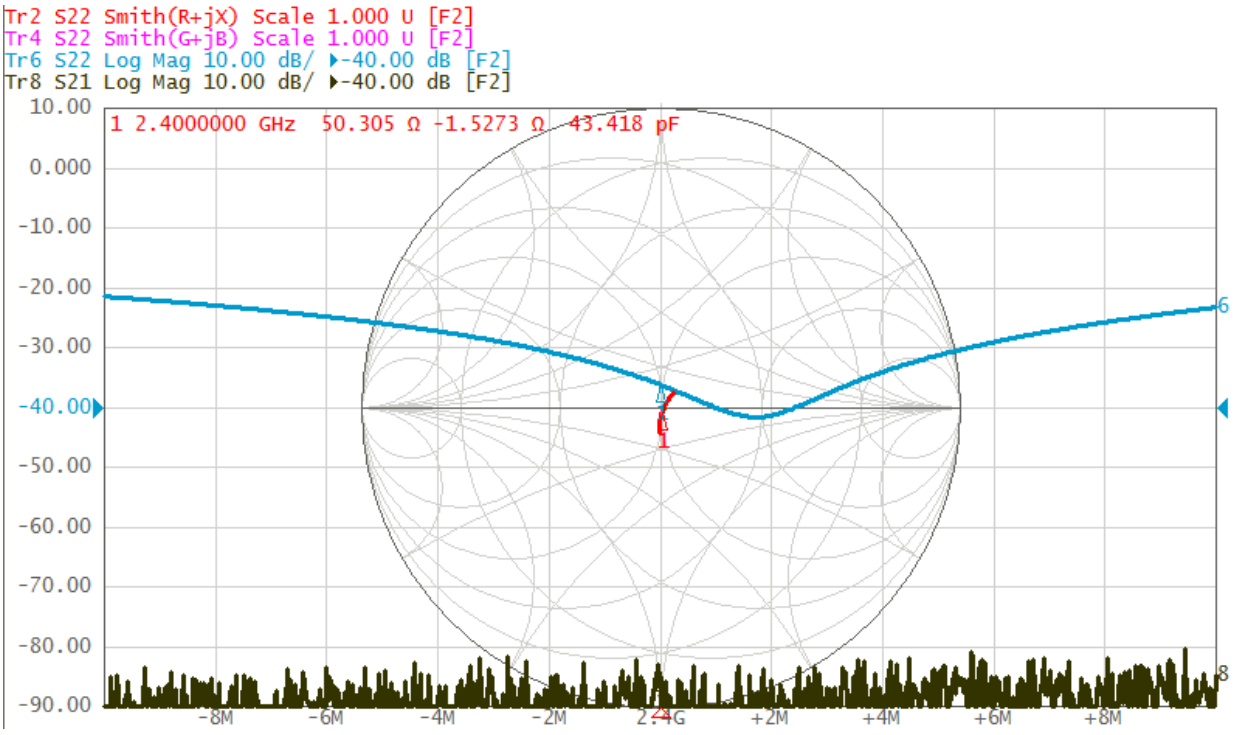

Figure 24. Experiment 5 port 2 results at 2.4 GHz.

The second experiment in concrete, experiment 6, was conducted with three couplers (two inline

and one perpendicular). The configuration was similar to the three-coupler in-air experiments. A standard 12 inch diameter by 48 inch long cardboard concrete form was again used with the same mix of concrete. The concrete was again allowed to cure for 12 days. The schematic and set-up for experiment 6 are shown in Figure 25. A picture of the experiment 6 concrete form during curing is shown in Figure 26. The VNA results at 2.4 GHz in configuration 1 are shown in Figure 27 for port 1 and Figure 28 for port 2. The VNA results for configurations 2 and 3, also at 2.4 GHz, are shown in Figures 29 through 32.

Like experiment 5, the results for experiment 6 also show poor insertion loss performance with no indication that any energy was transferred to or from either the inline or perpendicular couplers. The experiment 6 return loss results are not as good as the return loss results from experiment 5, showing just 10 to 13 dB of return loss. This is also reflected in the impedance measurements at the matched couplers which, as the data shows, were in the region of 60 + j 40 Ohms.

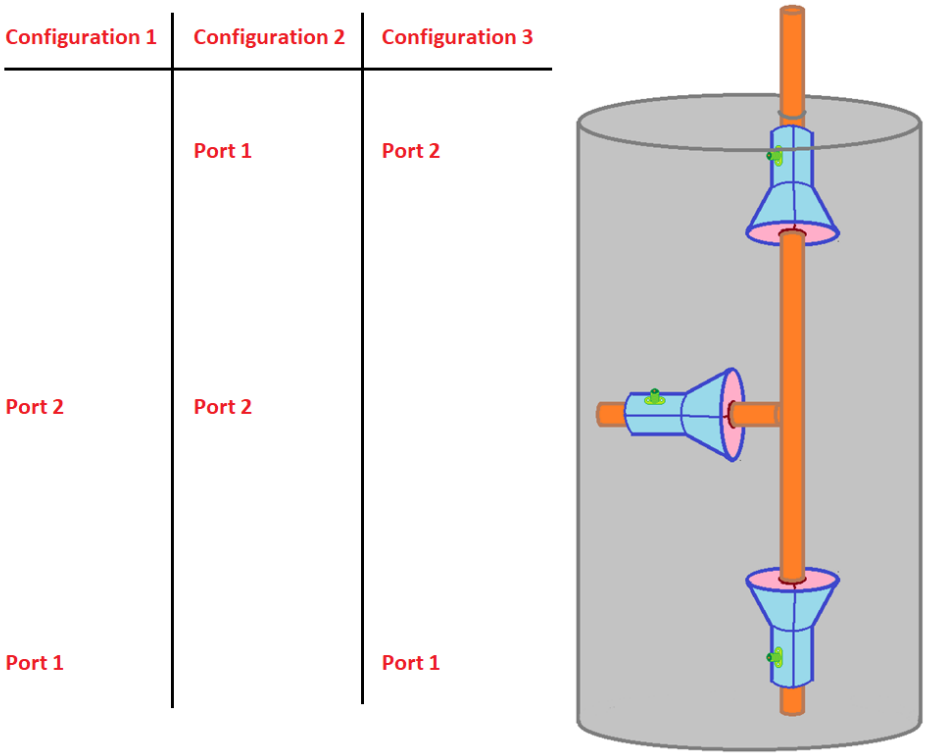

Figure 25. Experiment 6 schematic and set-up.

Figure 26. Experiment 6 concrete form during curing.

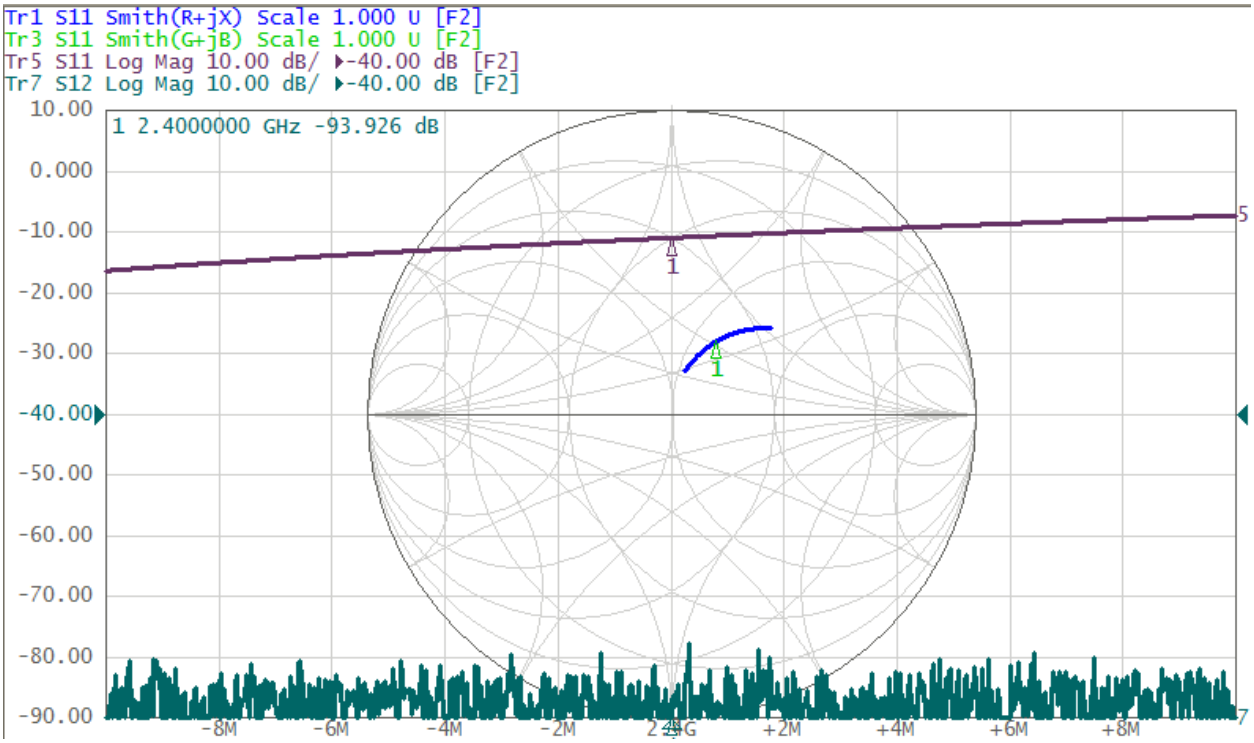

Figure 27. Experiment 6 results for port 1 and configuration 1.

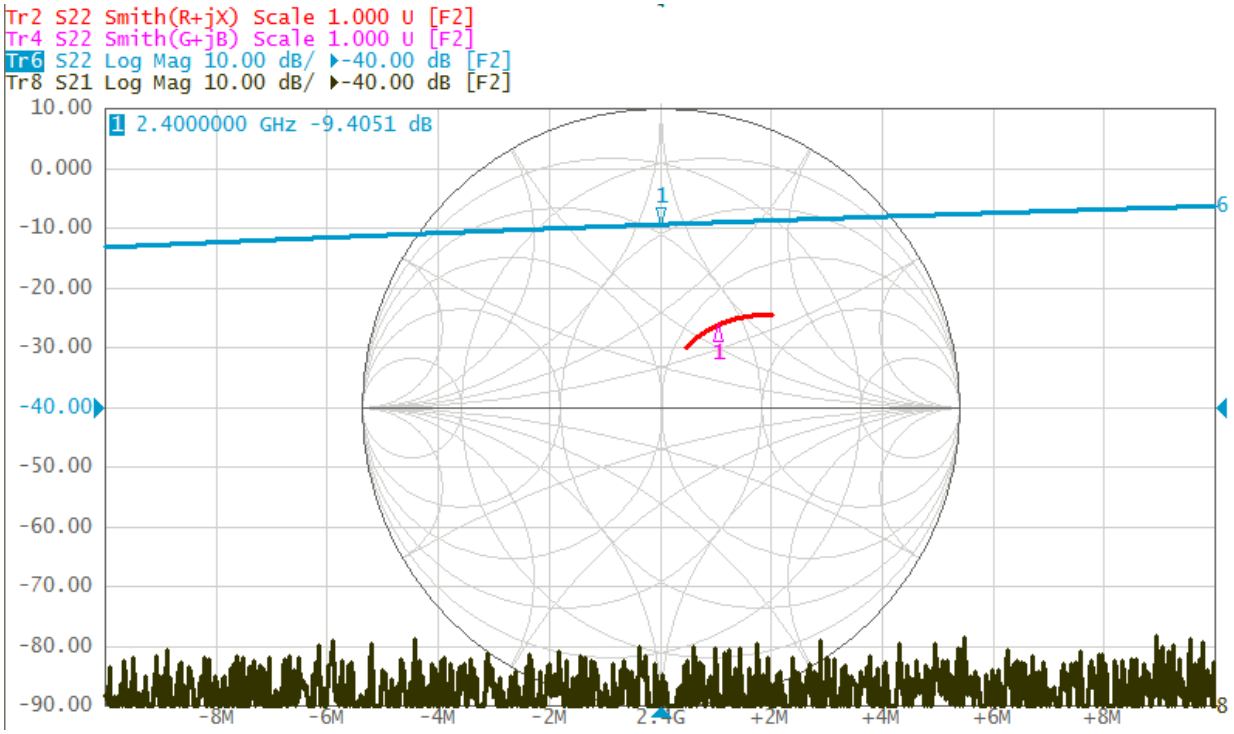

Figure 28. Experiment 6 results for port 2 and configuration 1.

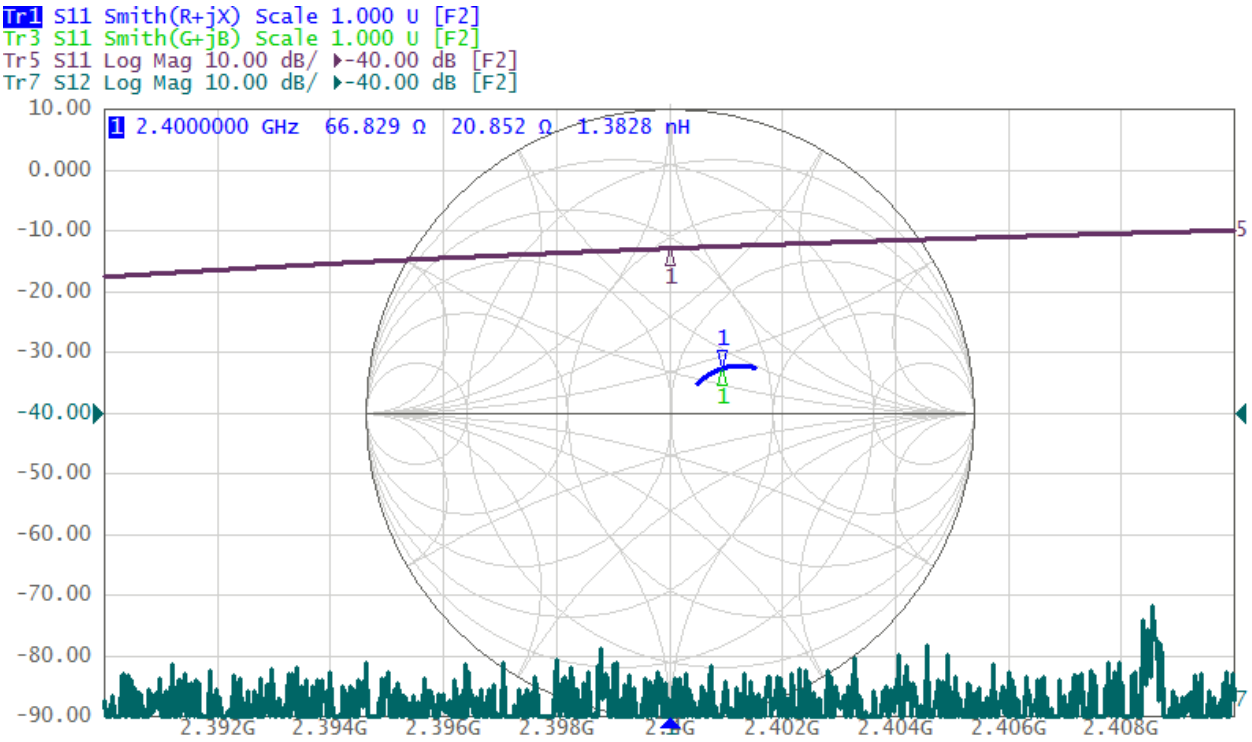

Figure 29. Experiment 6 results for port 1 and configuration 2.

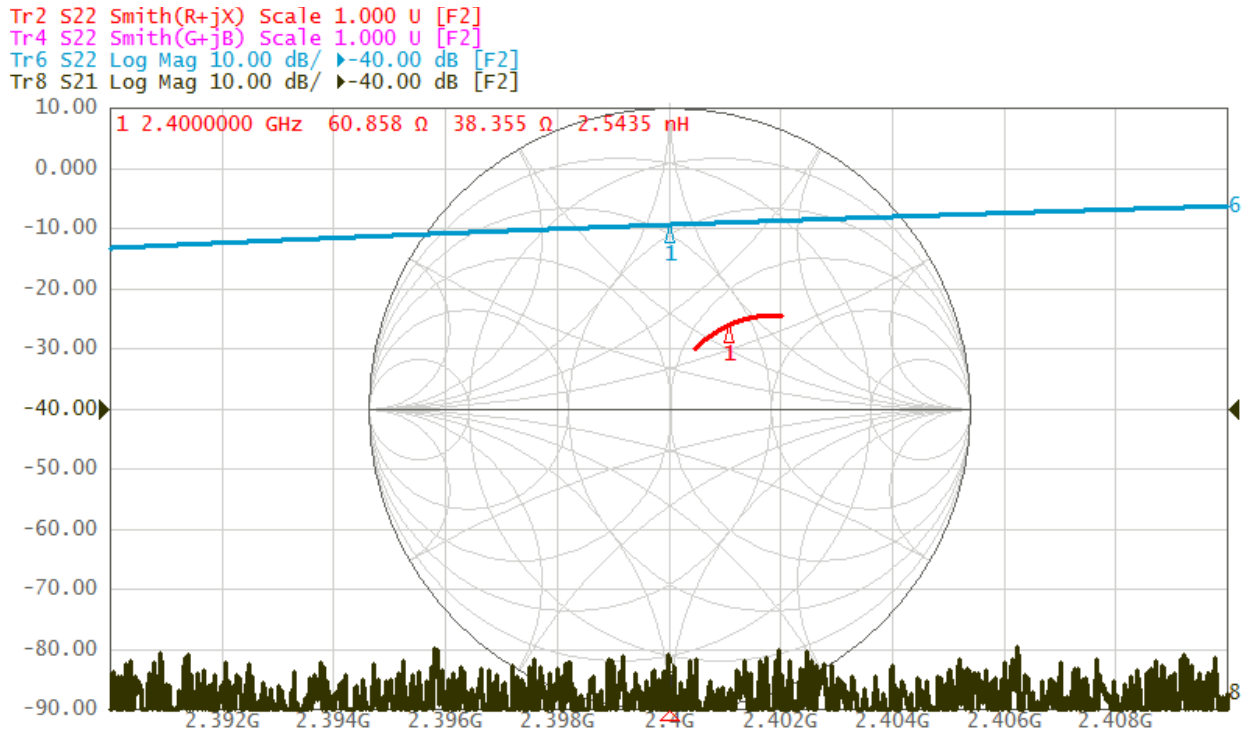

Figure 30. Experiment 6 results for port 2 and configuration 2.

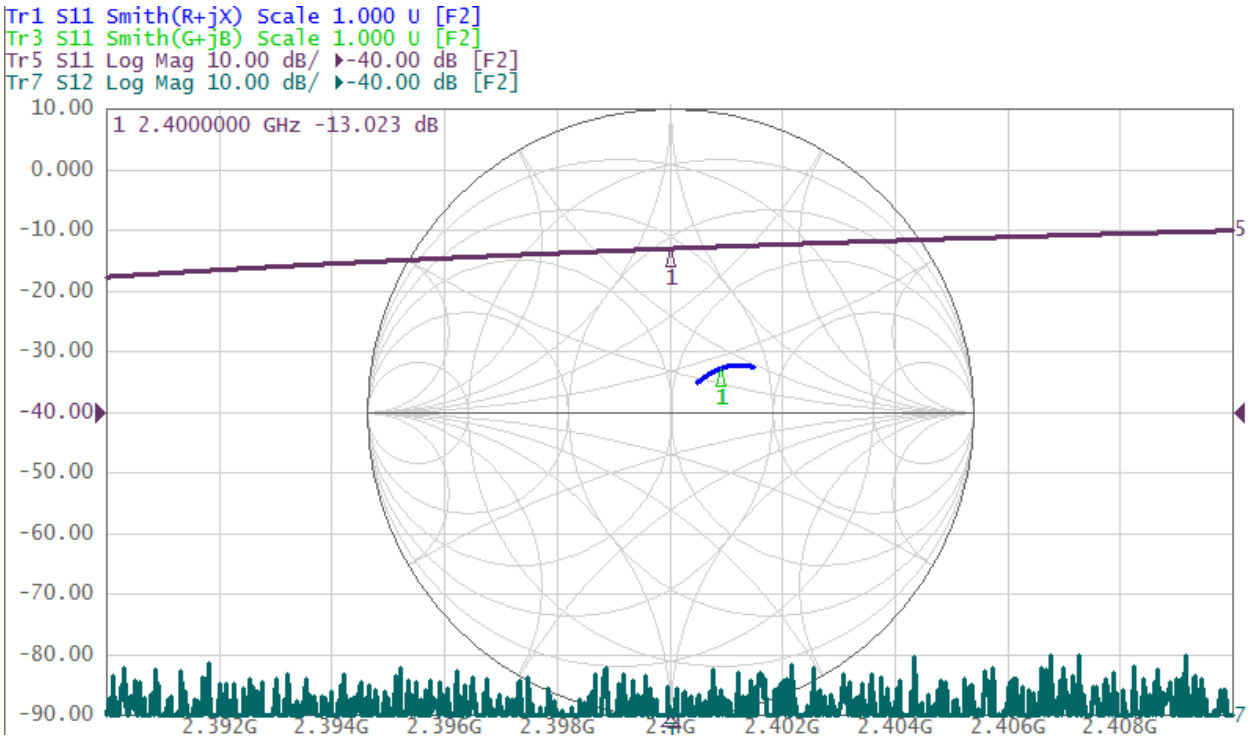

Figure 31. Experiment 6 results for port 1 and configuration 3.

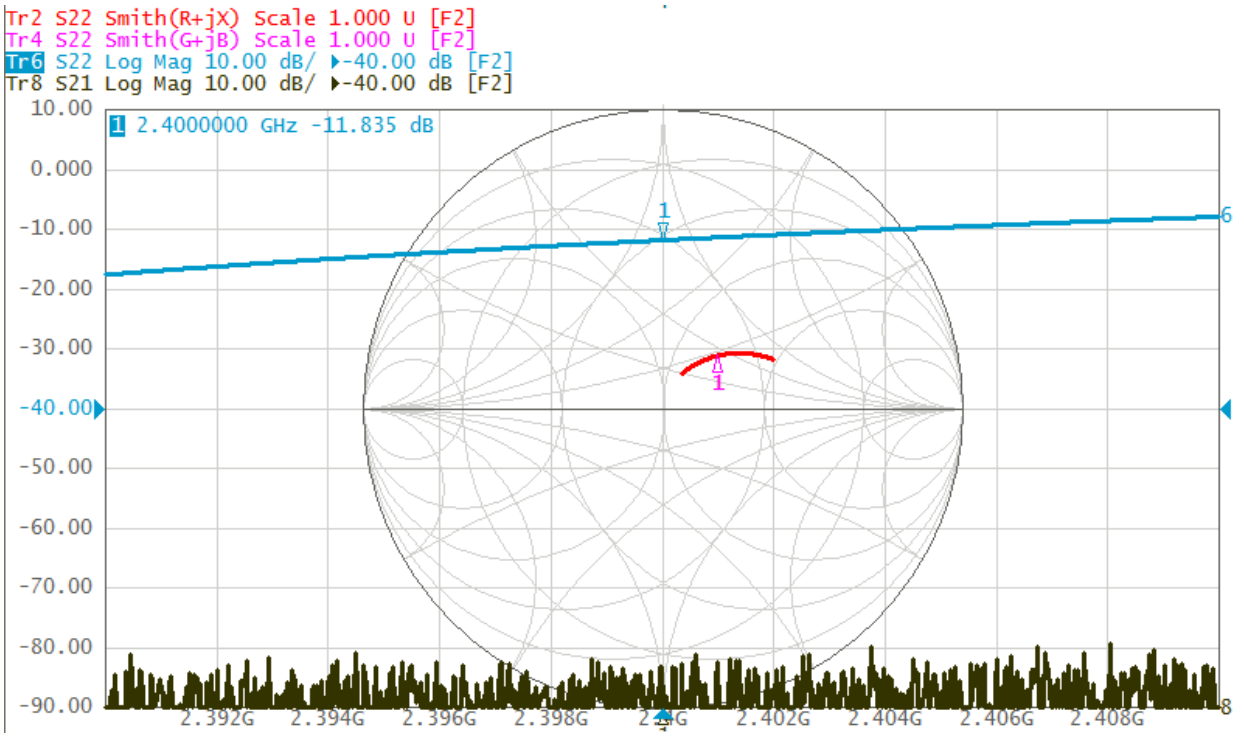

Figure 32. Experiment 6 results for port 2 and configuration 3.

CHAPTER 8. SINGLE WIRE TRANSMISSION LINE DESIGN 2

After reviewing the results of the experiments in design 1 which operated at 2.4 GHz it was theorized that either the moisture in the concrete or the dense composition of the concrete itself were hindering the single wire transmission process. It was reasoned that if radio frequency attenuation was the mechanism by which the propagation of the 2.4 GHz energy was being defeated then reducing the frequency may reduce the attenuation. Since the FCC governs all wireless (propagating) frequencies above 9 kHz, a frequency of 8 kHz was chosen for a second set of tests. If these experiments proved successful it was reasoned that there would be no regulatory issues with implementing the solution.

These experiments did not involve the use of directional couplers since the wavelength of 8 kHz in air is 37.5 kilometers long. In these experiments a simple coupling technique was employed where a single conductor was coupled to the rebar using a standard ground-bar grounding clamp. No return conductor was attached to the rebar or concrete. In fact, even the test stand interface was isolated from power ground using a charged, unplugged, uninterruptible power supply for the equipment at one end of the test to ensure a return path was not created through the test equipment.

CHAPTER 9. SINGLE WIRE TRANSMISSION LINE DESIGN 2 TESTING

The first experiment of design 2, experiment 7, tested a rebar structure in air. The structure was made of four straight pieces of rebar held in a column configuration by six round rebar rings. The rings were attached to the straight pieces using typical figure-eight rebar wire wraps. The straight segments are approximately 122 cm long number 5 rebar. The rings are smaller rebar, approximately 20.5 cm in diameter with several centimeters of overlap for the ends. Three test wires were clamped to the rebar, (two inline and one on a ring mid-way down the column structure). One end of the structure with a wire clamp installed can be seen in Figure 33. The experiment was implemented using a signal generator and a spectrum analyzer as show in Figure 34. The ground leads on both the signal generator and the spectrum analyzer were left disconnected. Experiment 7 was conducted with the rebar structure placed on a wooden bench.

For the second experiment, experiment 8, the rebar structure was encased in concrete. The same test configuration was implemented. The encased structure was stood on end on a wooden pallet for experiment 8. The experiment 8 set-up is shown in Figure 35. The test wires can be seen hanging from the side of the cardboard concrete form.

The test results for experiments 7 and 8 are shown together in Figure 36. While the power loss (insertion loss) is low in air, between approximately 18.5 and 24.75 dB, the loss in concrete is very high, between approximately 54.5 and 60.3 dB.

Figure 33. Experiment 7 set-up.

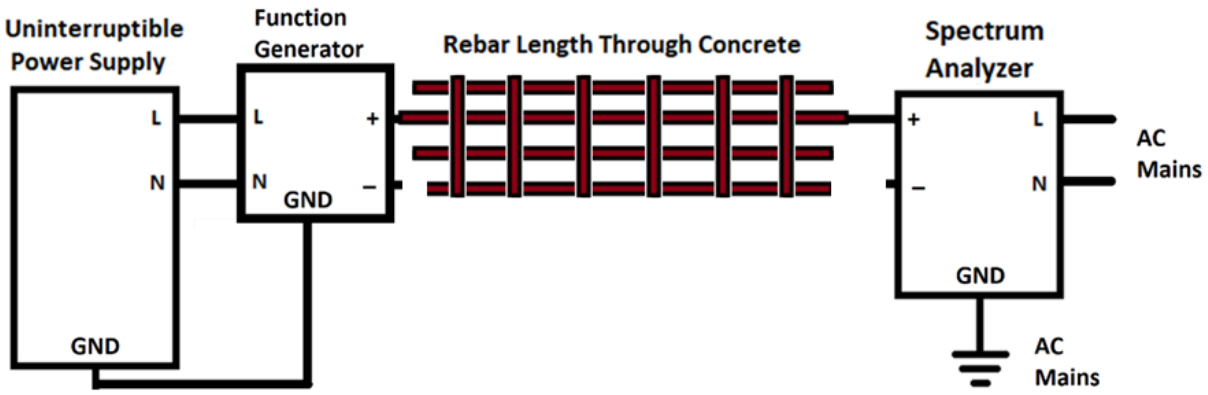

Figure 34. Experiment 7 schematic.

Figure 35. Experiment 8 set-up.

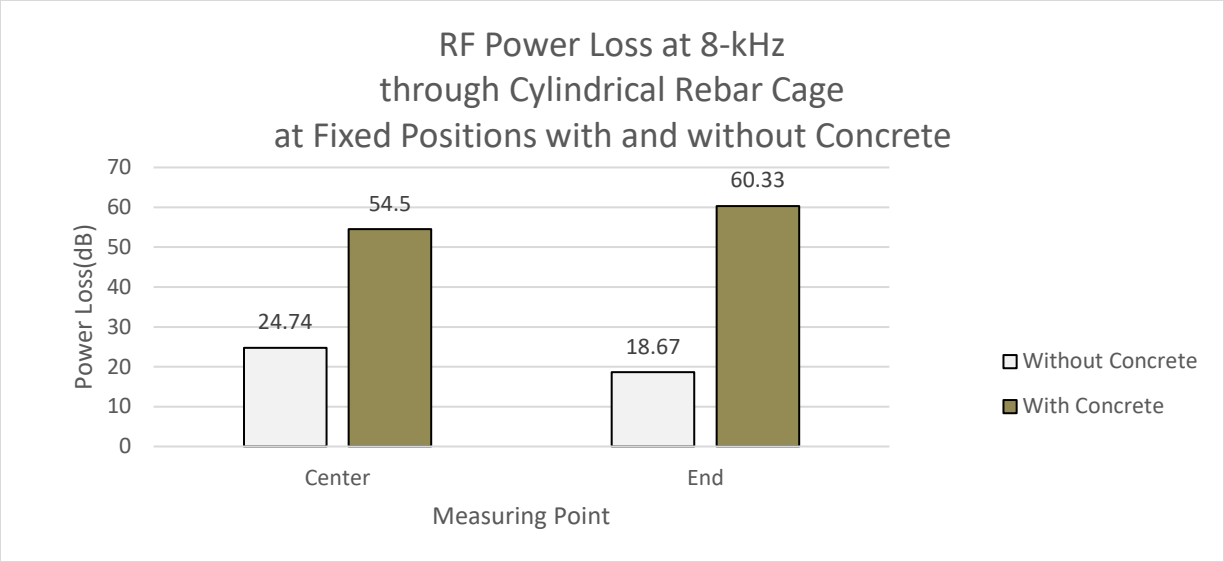

Figure 36. Results for experiments 7 and 8.

CHAPTER 10. CONCLUSIONS

The project tasks were completed and some results were favorable, though the desired goal of implementing both an energy harvesting and communication solution for embedded corrosion sensors in reinforced concrete was not obtained. An extensive literature search was conducted on the topics of corrosion sensing as well as energy harvesting and communications and a candidate technology was identified that had the potential to support both the delivery of energy to, and communications with the sensor. The identified technology was the single wire transmission line concept. Electromagnetic couplers that attach to the reinforcing steel and implement the single ire transmission line were developed as well as impedance matching circuits for the couplers. Laboratory experiments were then conducted first in air to baseline the approach and then in concrete. A second design approach, operating at a much lower frequency, was added after the results from the first experiment proved disappointing.

For the first design and set of tests, the baseline experiments in air were successful and validated the single wire transmission line design approach and coupler design. The experiments in air performed better than traditional wireless free space transmissions by a factor of 70. The impedance matching circuit designs also proved successful and worked well in air and even better in concrete. In air, the impedance matching circuit reduced the return losses to an acceptable level of below 18 dB and in concrete the return loss was better than 25 dB. The improvement may be due to the PVC-concrete interface at the conical end of the coupler being more closely matched than the PVC-air interface in the baseline experiments.

Unfortunately, when the experimental medium was changed from air to concrete the propagation performance deteriorated significantly. In fact, the insertion loss for radio frequency energy transmission in reinforced concrete using rebar as a single wire transmission line may be too low to be of use for energy harvesting or communications at 2.4 GHz. The insertion loss over a short distance of just over a meter, for 2.4 GHz, was too low to measure. During the second set of tests, at a much lower frequency of 8 kHz the insertion loss was measurable but still very large, between 54 and 60 dB over short distances on the order of a meter. While this may prohibit its use for energy harvesting it may still be possible to use the second design approach for communications on smaller foundations. Unfortunately, without an “unwired” solution for energy harvesting, solving only the communications problem does not offer significant advantages.

There are several future areas of work to consider in advancing this research. First, the success of the baseline experiments in air suggests that it may be possible to apply the single wire transmission line technique to stand-alone metal structures in air such as bridges, towers, or I-beams in buildings. While this technique may not be appropriate for new metal structures where sensor wiring can be included in the design, on an existing structure it may be possible to use the structure itself as a single wire transmission line to energize and communicate with structural monitoring sensors.

Regarding reinforced concrete corrosion monitoring, for those unique foundations that include concentric reinforced steel cages or a beam in the center of the pier, it may be possible to leverage the research on the lower frequency technique in the second design approach. If the two

steel structures can be electrically isolated from each other, then it may be possible to use the two separate structures in the concrete to form a two-wire circuit to both energize and communicate with embedded sensors. Embedded sensors would be connected between the two structures at various depths keeping wiring to a minimum. It is recognized that electrically isolating the two structures may cause concerns for grounding and also that the FDOT makes limited use of such unique steel structures in their foundation designs.

REFERENCES

[1] Ha-Won Song and Vela Saraswathy, “Corrosion Monitoring of Reinforced Concrete Structures – A Review”, *International Journal of Electrochemical Science*, Volume 2, January, 2007, pgs. 1-28.

[2] S. P. Karthick, S. Muralidharam, V. Saraswathy, and K. Thangavel, “Long-Term relative performance of embedded sensor and surface mounted electrode for corrosion monitoring of steel in concrete structures”, *Sensors and Actuators B: Chemical*, Volume 192, March, 2014, pgs. 303-309.

[3] Monzer M. Krishan, “Sensor Development for Corrosion Monitoring of Reinforcement Steel”, *International Journal of Scientific & Engineering Research,* Volume 6, February, 2015, pgs. 632-637.

[4] Guofu Qiao, Goudong Sun, Yi Hong, Tiejun Liu, and Xinchun Guan, “Corrosion in Reinforced Concrete Panels: Wireless Monitoring and Wavelet-Based Analysis”, *Sensors*, Volume 14, February, 2014, pgs. 3395-3407.

[5] Guofu Qiao, Goudong Sun, Yi Hong, Yuelan Qiu, and Jinping Ou, “Remote corrosion monitoring of the RC structures using the electrochemical wireless energy-harvesting sensors and networks”, *Nondestructive Testing and Evaluation (NDT&E) International*, Volume 44, November, 2011, pgs. 583-588.

[6] Muhammad Imran Khan, Abdul Mannan Khan, Ahmed Nouman, Muhammad Irfan Azhar, and Muhammad Khurram Saleem, “pH Sensing Materials for MEMS Sensors and Detection Techniques”, 2012 International Conference on Solid-State and Integrated Circuits (ICSIC), Published in the *International Proceedings of Computer Science and Information Technology (IPCSIT)*, Volume 32, 2012, pgs. 18-22.

[7] Rund J. M. Vullers, Rob van Schaijk, Hubregt J. Visser, Julien Penders, and Chris Van Hoof, “Energy Harvesting for Autonomous Wireless Sensor Networks”, *Current Science*, Volume 108, May, 2015, pgs. 1890-1900.

[8] Christopher R. Valenta and Gregory D. Durgin, “Harvesting Wireless Power”, *IEEE Microwave Magazine*, Volume 15, June, 2014, pgs. 108-120.

[9] Tolga Soyata, Lucian Copeland, and Wendi Heinzelman, “RF Energy Harvesting for Embedded Systems: A Survey of Tradeoffs and Methodology”, *IEEE Circuits and Systems Magazine*, Volume 16, January 2016, pgs. 22-57.

[10] Vijay Raghunathan and Pai H. Chou, “Design and Power Management of Energy Harvesting Embedded Systems”, Proceedings of the 2006 International Symposium on Low Power Electronics and Design, Tegernsee, Germany, October 4-6, 2006, pgs. 369-374.

[11] Sravanthi Chalasani and James M. Conrad, “A Survey of Energy Harvesting Sources for Embedded Systems”, Proceedings of the 2008 IEEE SoutheastCon, Huntsville, Alabama, April 3-6, 2008, pgs. 442-447.

[12] Sujesha Sudevalayam and Purushottam Kulkami, “Energy Harvesting Sensor Nodes: Survey and Implications”, *IEEE Communications Surveys & Tutorials,* Volume 13, September 2011, pgs. 443-461.

[13] Meng-Lin Ku, Wei Li, Yan Chen, and K.J. Ray Liu, “Advances in Energy Harvesting Communications: Past, Present, and Future Challenges”, *IEEE Communications Surveys & Tutorials,* Volume 18, April 2016, pgs. 1384-1412.

[14] Venkatesha Prasad, Shruti Devasenapathy, Vijay S. Rao, and Javad Vazifehdan, “Reincarnation in the Ambiance: Devices and Networks with Energy Harvesting”, *IEEE Communications Surveys & Tutorials,* Volume 16, January 2014, pgs. 195-213.

[15] Guodong Sun, Guofu Qiao, and Bin Xu, “Corrosion Monitoring Sensor Networks With Energy Harvesting”, *IEEE Sensors Journal,* Volume 11, June 2011, pgs. 1476-1477.

[16] Lina Mohjazi, Mehrdad Dianati, George K. Karagiannidis, Sami Muhaidat, and Mahmoud Al-Qutayri, “RF-Powered Cognitive Radio Networks: Technical Challenges and Limitations”, *IEEE Communications Magazine*, Volume 53, April 2015, pgs. 94-100.

[17] Rong Zhang, Robert G. Maunder, and Lajos Hanzo, “Wireless Information and Power Transfer: From Scientific Hypothesis to Engineering Practice”, *IEEE Communications Magazine*, Volume 53, August 2015, pgs. 99-105.

[18] Parisa Ramezani and Mohammad Reza Pakravan, “Overview of MAC Protocols for Energy Harvesting Wireless Sensor Networks”, 26th IEEE Symposium on Personal, Indoor and Mobile Radio Communications, Hong Kong, China, August 30 – September 2, 2015, pgs. 2032-2037.

[19] Fan Zhang and Vincent K. N. Lau, “Delay-Sensitive Dynamic Resource Control for Energy Harvesting Wireless Systems with Finite Energy Storage”, *IEEE Communications Magazine,* Volume 53, August 2015, pgs. 106-113.

[20] Omur Ozel, Kaya Tutuncuoglu, Sennur Ulukus, and Aylin Yener, “Fundamental Limits of Energy Harvesting Communications”, *IEEE Communications Magazine,* Volume 53, April 2015, pgs. 126-132.

[21] Winston K. G. Seah, Zhi Ang Eu, and Hwee-Pink Tan, “Wireless Sensor Networks Powered by Ambient Energy Harvesting (WSN-HEAP) – Survey and Challenges”, First International Conference on Wireless Communications, Vehicular Technology, Information Theory and Aerospace & Electronic Systems Technology, Aalborg, Denmark, May 17-20, 2009, pgs. 1-5.

[22] Xiao Lu, Ping Wang, Dusit Niyato, Dong In Kim, and Zhu Han, “Wireless Networks With RF Energy Harvesting: A Contemporary Survey”, *IEEE Communications Surveys & Tutorials,* Volume 17, April 2015, pgs. 757-789.

[23] Benton H. Calhoun, Denis C. Daly, Naveen Verma, Daviel F. Finchelstein, David D/ Wentzloff, Alice Wang, Seong-Hwan Cho, and Anantha P. Chandrakasan, “Design Considerations for Ultra-Low Energy Wireless Microsensor Nodes”, *IEEE Transactions on Computers*, Volume 54, June 2005, pgs. 727-740.

[24] William Marion and Stephen Wilcox, *Solar Radiation Data Manual for Flat-Plate and Concentrating Collectors*, National Renewal Energy Laboratory, United States Department of Energy, Boulder Colorado, March 1994.

[25] Peter J. Cousins, David D. Smith, Hsin- Chiao Luan, Jane Manning, Tim D. Dennis, Ann Waldhauer, Karen E. Wilson, Gabriel Harley and William P. Mulligan, "Generation 3: Improved performance at lower cost", Proceedings of the 35th IEEE Photovoltaic Specialists Conference, Honolulu, Hawaii, June 20-25, 2010, pgs. 275-278.

[26] William C. Stone, *NIST Construction Automation Program Report No. 3 Electromagnetic Signal Attenuation in Construction Materials* (Report Number NISTIR 6055), Building and Fire Research Laboratory, National Institute of Standards and Technology, Gaithersburg, Maryland, October 1997, pgs. 171-177.

[27] Shan Jiang and Stavros Georgakopoulos, " Electromagnetic Wave Propagation into Fresh Water ", *Journal of Electromagnetic Analysis and Applications*, 2011, Number 3, pgs. 261-266.

[28] E. J. Hilliard, *Electromagnetic Radiation in Seawater* (Report Number 316), U.S. Naval Underwater Ordinance Station, Newport, Rhode Island, Revised August, 1960.

[29] M.N. Soutsos, J.H. Bungey, SW.G. Millard, M.R. Shaw, A. Patterson, "Dielectric Properties of Concrete and Their Influence on Radar Testing", *Non-Destructive Testing and Evaluation International*, Volume 34, Number 6, September 2001, pgs. 419-425.

[30] Antoine Robert, "Dielectric permittivity of concrete between 50 Mhz and 1 Ghz and GPR measurements for building materials evaluation", *Journal of Applied Geophysics*, Volume 40, Issues 1-3, October 1998. pgs. 89–94.

[31] Arnold Sommerfeld, "Ueber die Fortpflanzung elektrodynamischer Wellen langs eines Drahtes", *Annalen Der Physik Und Chemie*, Issue Number 2, 1899, pgs. 233-290, as translated by Google, April 4, 2017.

[32] Georg Goubau, "Open Wire Lines", *IRE Transactions on Microwaves and Techniques*, October, 1956, pgs. 197-200.

[33] John A. Richards, *Radio Wave Propagation*, Springer-Verlag, Berlin-Heidelberg, 2008, pg. 88.

[34] H. A. Scarton, K. R. Wilt, and G. J. Saulnier, "Ultrasonic Communications Through a Reinforced Concrete Column", Proceedings of the ASME 2016 International Mechanical Engineering Congress and Exposition, Volume 13, Acoustics, Vibration, and Wave Propagation, Phoenix, Arizona, November 11-17, 2016.

[35] G. Elmore, "Introduction to the Propagating Wave on a Single Conductor," Corridor Systems Inc., Santa Rosa, California, 2009.

[36] G. J. Goubau, "Single-Conductor Surface-Wave Transmission Lines," *Proceedings of the I.R.E.*, June 1951, pp. 619-624.

[37] C.E. Sharp, and G. Goubau, “ A UHF Surface Wave Transmission Line”, *Proceedings of the I.R.E.,* January 1953, pp. 107-109.

[38] G. J. Goubau, "Surface Waves and Their Application to Transmission Lines," *Journal of Applied Physics,* Vol. 21, November, 1950, pp. 1119-1128.

APPENDIX 1. FIELD STRENGTH MEASUREMENTS

Electric and Magnetic field strength measurements were made along the length of the rebar with a transmitting and receiving 2.4 GHz couplers installed with matching circuits. The distance between the couplers was set at approximately nine wavelengths or 110.5 cm. Magnetic and electric field probes were positioned above the rebar (one at a time) and moved linearly along the rebar. Field strength measurements were recorded and graphed. The probe set-up includes a Bee-Hive Electronics Series 100 Electromagnetic Compliance (EMC) probe set and a Series 150 EMC amplifier. The amplifier output was connected to a spectrum analyzer where the measurements were made. The lab set-up is shown in Figure A-1. The long and narrow yellow electric field probe is pointing down with the tip just above the rebar.

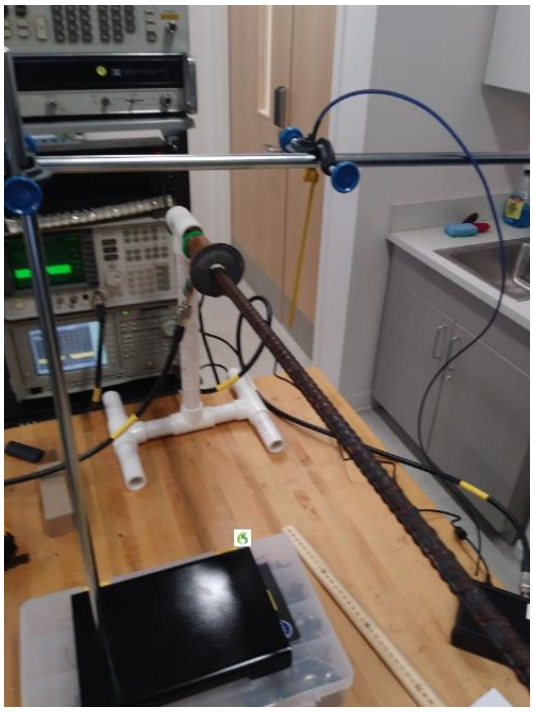

Figure A-1. Field Strength Measurement Lab Set-up.

The transmitting coupler was attached to a 20 dBm source at 2.4 GHz and the receiving coupler was terminated into 50 Ohms. Both magnetic and electric field strength measurements were taken along the rebar at a height of 2.56 cm above the center of the rebar. Subsequently, magnetic field strength measurements were also taken at a farther distance of 7.24 cm above the center of the rebar. The magnetic field strength measured at lateral distances from the transmitting coupler are shown in Figure A-2.

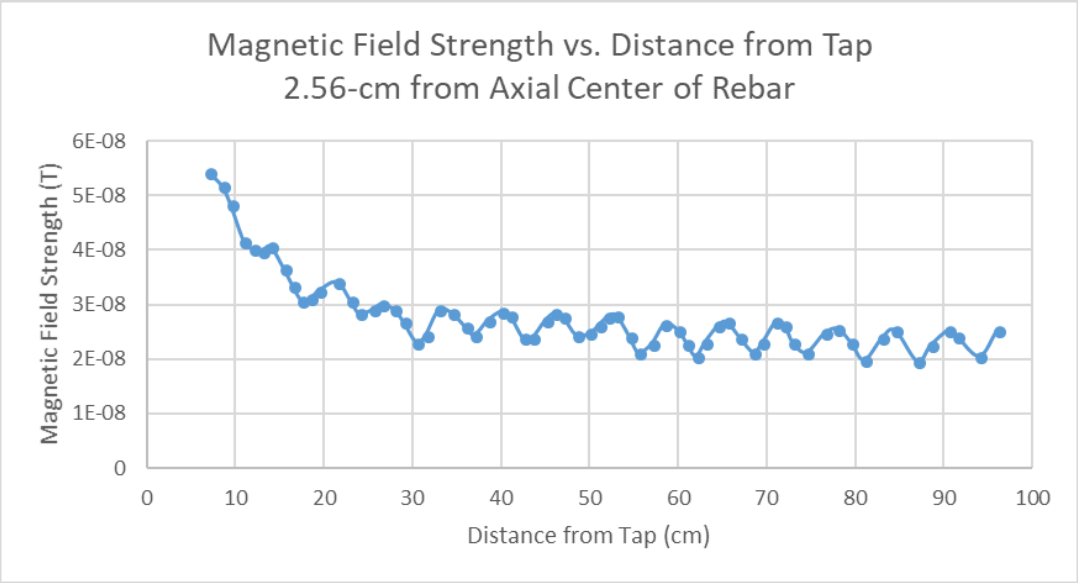

Figure A-2. Magnetic field strength at a vertical distance of 2.56 cm.

The magnetic field strength data has been converted to units of Tesla using Bee Hive Electronics Series 150 EMC amplifier conversion scales. The electric field strength data at the vertical distance of 2.56 cm is shown in Figure A-3. The magnetic field strength test was also repeated at a distance of 7.24 cm. That data is included in Figure A-4. It can be seen in all of the plots that the distance between the field strength peaks is approximately 6-7 cm. Recalling that a half wavelength is 6.25 cm the distance between peaks is not unexpected. In addition, the difference in the magnetic field strength is proportional to the inverse of the increase in distance. This follows from applying Ampere's law to a long straight conductor. It must be noted that all of these measurements were conducted within small, sub-wavelength, distances of the couplers and the rebar. This means that some non-linear near-field effects are also present. This does not negate the results but their precision may not be reliable. In any event, the purpose of this study was to reveal something about the geometry of the electric, and especially the magnetic fields near the rebar which was achieved. The results suggest that a spacing of a multiple of wavelengths should suffice for the experiments.

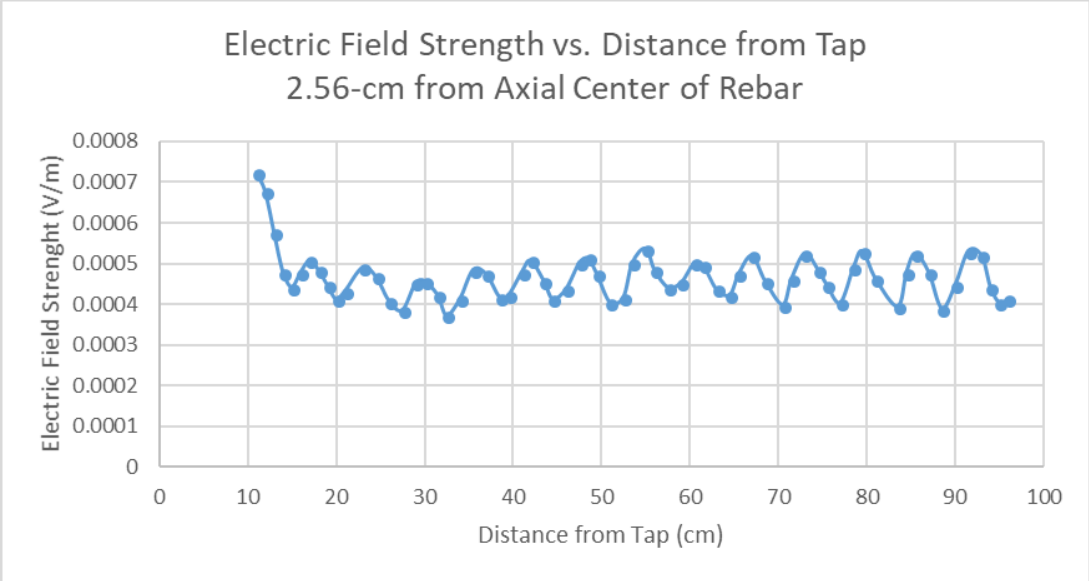

Figure A-3. Electric field strength at a vertical distance of 2.56 cm.

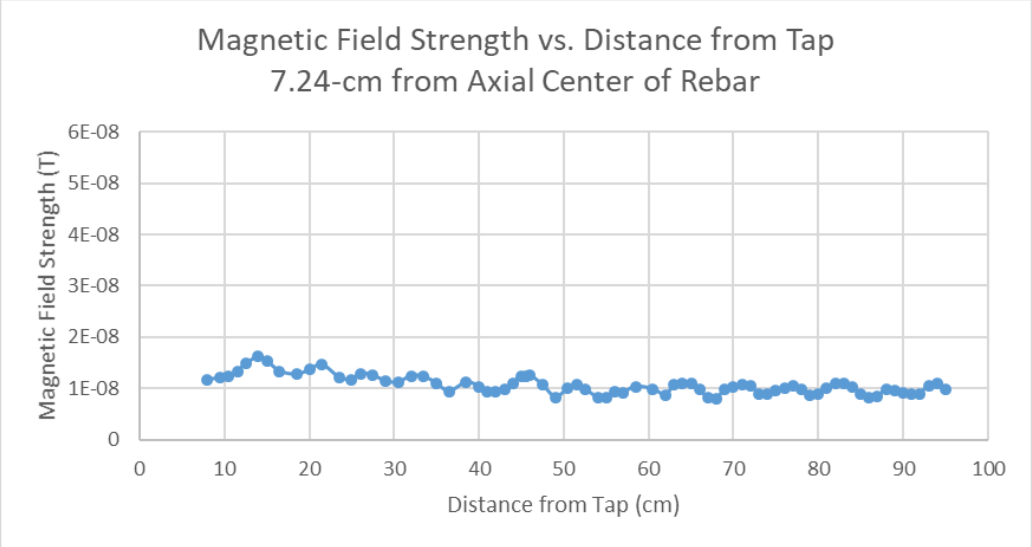

Figure A-4. Magnetic field strength at a vertical distance of 7.24 cm.